

# Journal Pre-proof

Design and structural optimization of novel 2*H*-benzo[h]chromene derivatives that target AcrB and reverse bacterial multidrug resistance

Yinhu Wang, Rawaf Alenazy, Xinjie Gu, Steven W. Polyak, Panpan Zhang, Matthew J. Sykes, Na Zhang, Henrietta Venter, Shutao Ma



PII: S0223-5234(20)31021-7

DOI: <https://doi.org/10.1016/j.ejmech.2020.113049>

Reference: EJMECH 113049

To appear in: *European Journal of Medicinal Chemistry*

Received Date: 28 August 2020

Revised Date: 21 October 2020

Accepted Date: 23 November 2020

Please cite this article as: Y. Wang, R. Alenazy, X. Gu, S.W Polyak, P. Zhang, M.J. Sykes, N. Zhang, H. Venter, S. Ma, Design and structural optimization of novel 2*H*-benzo[h]chromene derivatives that target AcrB and reverse bacterial multidrug resistance, *European Journal of Medicinal Chemistry*, <https://doi.org/10.1016/j.ejmech.2020.113049>.

This is a PDF file of an article that has undergone enhancements after acceptance, such as the addition of a cover page and metadata, and formatting for readability, but it is not yet the definitive version of record. This version will undergo additional copyediting, typesetting and review before it is published in its final form, but we are providing this version to give early visibility of the article. Please note that, during the production process, errors may be discovered which could affect the content, and all legal disclaimers that apply to the journal pertain.

© 2020 Elsevier Masson SAS. All rights reserved.

## Graphical Abstract:

## Design and structural optimization of novel 2*H*-benzo[*h*]chromene derivatives that target AcrB and reverse bacterial multidrug resistance

Yinhu Wang<sup>a,b,1</sup>, Rawaf Alenazy<sup>c,d,1</sup>, Xinjie Gu<sup>a</sup>, Steven W Polyak<sup>c</sup>, Panpan Zhang<sup>a</sup>, Matthew J. Sykes<sup>c</sup>, Na Zhang<sup>a</sup>, Henrietta Venter<sup>c,\*</sup>, Shutao Ma<sup>a,\*</sup>

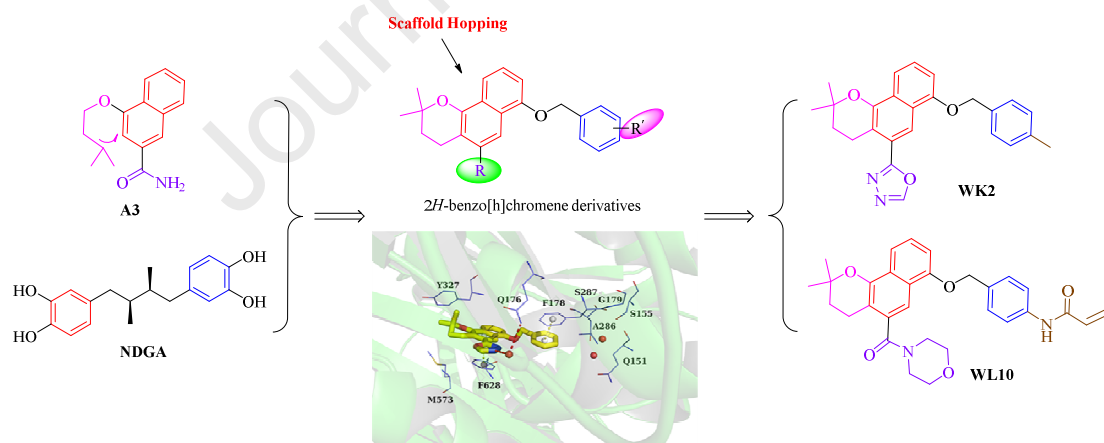
<sup>a</sup>Department of Medicinal Chemistry, Key Laboratory of Chemical Biology (Ministry of Education), School of Pharmaceutical Sciences, Cheeloo College of Medicine, Shandong University, 44 West Wenhua Road, Jinan 250012, China

<sup>b</sup>School of Pharmacy, Liaocheng University, Liaocheng, China

<sup>c</sup>Clinical and Health Sciences, University of South Australia, Adelaide, SA 5000, Australia

<sup>d</sup>Department of Medical Laboratory, College of Applied Medical Sciences-Shaqra, Shaqra University, 11961, Saudi Arabia

Novel chromanone and benzo[*h*]chromene derivatives were designed, synthesized and evaluated as AcrB inhibitors.



## Design and structural optimization of novel 2*H*-benzo[h]chromene derivatives that target AcrB and reverse bacterial multidrug resistance

Yinhu Wang<sup>a,b,1</sup>, Rawaf Alenazy<sup>c,d,1</sup>, Xinjie Gu<sup>a</sup>, Steven W Polyak<sup>c</sup>, Panpan Zhang<sup>a</sup>, Matthew J. Sykes<sup>c</sup>, Na Zhang<sup>a</sup>, Henrietta Venter<sup>c,\*</sup>, Shutao Ma<sup>a,\*</sup>

<sup>a</sup>*Department of Medicinal Chemistry, Key Laboratory of Chemical Biology (Ministry of Education), School of Pharmaceutical Sciences, Cheeloo College of Medicine, Shandong University, 44 West Wenhua Road, Jinan 250012, China*

<sup>b</sup>*School of Pharmacy, Liaocheng University, Liaocheng, China*

<sup>c</sup>*Clinical and Health Sciences, University of South Australia, Adelaide, SA 5000, Australia*

<sup>d</sup>*Department of Medical Laboratory, College of Applied Medical Sciences-Shaqra, Shaqra University, 11961, Saudi Arabia*

\*Corresponding authors.

*E-mail addresses:* mashutao@sdu.edu.cn (S. Ma); rietie.venter@unisa.edu.au (H. Venter).

<sup>1</sup>These authors contributed equally

Running title: 2*H*-Benzo[h]chromenes derivatives as AcrB inhibitors

**Abstract:** Drug efflux pumps have emerged as a new drug targets for the treatment of bacterial infections in view of its critical role in promoting multidrug resistance. Herein, novel chromanone and 2*H*-benzo[h]chromene derivatives were designed by means of integrated molecular design and structure-based pharmacophore modeling in an attempt to identify improved efflux pump inhibitors that target *Escherichia coli* AcrB. The compounds were tested for their efflux inhibitory activity, ability to inhibit efflux, and the effect on bacterial outer and inner membranes. Twenty-three novel structures were identified that synergized with antibacterials tested, inhibit Nile red efflux, and acted specifically on the AcrB. Among them, **WK2**, **WL7** and **WL10** exhibiting broad-spectrum and high-efficiency efflux inhibitory activity were identified as potential ideal AcrB inhibitors. Molecular modeling further revealed that the strong  $\pi$ - $\pi$  stacking interactions and hydrogen bond networks were the major contributors to tight binding of AcrB.

**Keywords:** 2*H*-Benzo[h]chromene; Multidrug resistance; AcrB inhibitors; Efflux inhibitory activity

## 1. Introduction

The decreasing efficacy of existing antibiotics for the treatment of infectious diseases caused by bacteria has accelerated worldwide in recent years [1, 2]. In particular, multidrug resistance (MDR) in pathogenic Gram-negative bacteria, including *Escherichia coli*, *Pseudomonas aeruginosa*, *Klebsiella pneumoniae*, and *Acinetobacter spp.*, poses a serious threat to global health as bacteria have acquired resistance mechanisms to one or more classes of clinically important antibiotics [3-6]. At present, approximately 700,000 people die of bacterial infections every year. It is estimated that by 2050 bacterial infections will cause 10 million deaths, and kill more people than cancer, if no action is taken to address MDR now [7]. Therefore, the discovery of novel antibacterials, or development of safe adjuvants that potentiate the activity of existing antibiotics, is urgently needed to avoid a return to the pre-antibiotic era [8].

Gram-negative bacteria are intrinsically resistant to many antibiotic classes due to the presence of a lipopolysaccharide rich outer membrane and multidrug efflux pumps [9, 10]. The highly impermeable outer membrane effectively restricts antibiotics from penetrating into bacteria, whilst efflux pumps recognize structurally distinct chemicals and extrude them from the cell before they can reach their intracellular drug targets and exert their antibacterial activity [11-14]. As a result, the development of therapeutic adjuvants that can inhibit the action of efflux pumps is a promising strategy to re-empower those antibacterials that are subject to efflux mechanisms [15-18]. Pharmacological efflux pump inhibitors (EPIs) have emerged as promising, alternative therapeutics that have the potential to improve antibacterial potency and reverse MDR [19, 20].

Over-expression of intrinsic efflux pump complexes is a primordial resistance mechanism that permits bacteria to survive when challenged with toxic chemicals [12, 21, 22]. One of the most widely studied and common efflux systems contributing to MDR in Gram negative bacteria is the tripartite AcrAB-TolC pump, which comprises an inner membrane transporter (AcrB), an outer membrane channel protein (TolC), and a periplasmic protein (AcrA) that connects AcrB and TolC [23-25]. AcrB catalyses drug/H<sup>+</sup> antiport and is the subunit responsible for selective substrate binding and expulsion, thus playing an essential role in the efflux mechanism [26, 27]. Crystal structures of AcrB in complex with natural substrates or small molecule EPIs have provided molecular details into the mechanisms of action and inhibition, respectively, that help to establish AcrB as a potential therapeutic target. Structural studies have revealed that AcrB assembles as a homotrimer, and substrates are transported through the protein using a rotational mechanism that requires co-operation between all three subunits. Compounds that inhibit one AcrB subunit consequentially impede the entire efflux machinery [28]. Structural studies have also identified an important inhibitor binding site, known as the hydrophobic trap, which is voluminous, flexible, and rich in aromatic amino-acid residues, such as Phe136, Phe178, Phe610, Phe615, Phe617 and Phe628. The phenylalanine rich pocket facilitates binding to a wide variety of hydrophobic substrates and EPIs via hydrophobic bonding and  $\pi$ - $\pi$  interactions [15, 19, 29-32]. In addition, certain polar residues, such as Asn274 and Gln176, provide further opportunities for hydrogen bonding, as do water molecules present in the substrate binding channel [29, 31]. Over the past decade, a number of AcrB inhibitors from different chemical classes have been discovered, including PA $\beta$ N, NMP, plumbagin and MBX3135 (Fig. 1). Recent crystal structures of AcrB in complex with MBX3135 and its derivatives have highlighted the critical role of Phe628 and Phe178 in the inhibition mechanism and provides valuable information for the design of new and more powerful EPIs [15, 19, 31]. To date, no EPIs have entered the clinic for various reasons, such as low chemical stability, poor selectivity for the bacterial drug target or high cytotoxicity. New EPIs with improved pharmacology or biological activity would be a welcome addition in the fight against MDR.

<Insert Fig. 1>

We have previously reported two novel classes of AcrB inhibitors, 2-naphthamide derivatives (**A3** and **7g**) [7, 33] and nordihydroguaiaretic acid (NDGA) derivatives (**NDGA** and **WD6**) (Fig. 1) [34, 35]. These representative compounds displayed promising activity as antibiotic potentiators against highly-drug resistant *E. coli*. Consequently, these EPIs have emerged as lead compounds due to their efflux inhibitory activity, novel drug-like scaffolds and favourable biological properties. In the current study we applied an integrated molecular design strategy to devise the synthesis of novel chromanone and 2*H*-benzo[h]chromene derivatives by fusing the structures of **A3**, **7g** and **WD6**. The ability of these compounds to potentiate the activity of antibiotics, to inhibit AcrB-mediated substrate efflux and to target AcrB specifically was systematically evaluated. Moreover, the structure-activity relationships (SARs) and molecular modeling were further investigated to explore the possible mechanisms of binding and inhibition against AcrB.

## 2. Results and discussion

### 2.1 Molecular design

Our previous docking experiments demonstrated that the naphthalene moiety of **A3** (Fig. 2a) and one benzene moiety of **WD6** (Fig. 2b) were both oriented parallel to the Phe628 side chain, resulting in extensive  $\pi$ - $\pi$  stacking interactions. The second benzene ring of **WD6** was also accommodated in the hydrophobic pocket through  $\pi$ - $\pi$  stacking interaction with Phe178 [33-35]. Thus, we proposed that our newly designed compounds should contain at least two appropriately spaced aromatic groups to force the necessary interactions with Phe628 and Phe178 simultaneously, resulting in tight binding with AcrB. In view of the above structural constraints, and to build upon our previous findings, two hypothetical pharmacophores for new AcrB EPIs were proposed based upon an integrated molecular design and scaffold hopping strategy (outlined in Fig. 2). We first replaced the naphthalene moiety of **A3** with a 2,2-dimethylchroman-4-one fragment, and integrated the benzene moiety of **WD6** to produce novel-structure chromanone derivatives (Fig. 2b). The benzene moiety was then derivatized for further bonding interactions. To verify the possible binding mode of the new derivatives, a molecular docking study was performed. As depicted in Fig. 2b, the structure of novel chromanone derivative retained the critical binding interactions observed in **A3** and **WD6**, namely (1) two aromatic rings for interaction with Phe628 and Phe178 and (2) a gemdimethyl group for additional hydrophobic interactions with Met573 and Tyr327.

Subsequently, we substituted the 2,2-dimethylchroman-4-one moiety with the 2*H*-benzo[h]chromene core with larger aromatic volume in order to obtain stronger  $\pi$ - $\pi$  interactions with Phe628. Inspection of the binding pocket revealed that a water molecule bound to Gln176 by a hydrogen bond was located near the C-5 position of the 2*H*-benzo[h]chromene core. Additionally, there was still sufficient space between the 2*H*-benzo[h]chromene core and the water molecule to accommodate larger groups. Therefore, further structural modification could be elaborated by introduction of certain polar substituents at the C-5 position of the 2*H*-benzo[h]chromene core to serve as hydrogen bond acceptors or donors and form additional hydrogen bonds with AcrB via water mediated interactions. Additionally, the large and flexible pocket consisting of Gln151, Ser155, Phe178, Gly179, Ala286, and Ser287, surrounded the benzene ring at the side chain end of the chromanone or 2*H*-benzo[h]chromene core, provided suitable space for introducing a variety of groups to the terminal benzene ring.

On the basis of the proposed binding modes described above, the 2*H*-benzo[h]chromene could be divided into two functional parts, as shown in Fig. 2c, R section as hydrogen-bond-forming “hydrophilic groups” and the R' section as “multi-functional groups”. In the R positions, polar groups (e.g. morpholinyl, oxadiazolyl, tetrazolyl, carboxyl, and hydrazide, etc.) that could form hydrogen bonds with resident water were preserved to improve the binding affinity for AcrB, whilst a variety of functional groups that could form hydrophobic contacts or hydrogen bonds with amino acid residues or water molecules were introduced at the R' positions. To identify more potent AcrB inhibitors for further pharmacological evaluation, as well as to verify the SARs, structural optimization was carried out through three chemical modifications: (1) hydrophilic modification on the 2*H*-benzo[h]chromene ring (R section), and (2) multi-functional modification on the benzene ring (R' section), and (3) scaffold hopping from chromanone core to 2*H*-benzo[h]chromene core.

<Insert Fig. 2>

## 2.2. Chemistry

The synthesis of a series of the chromanone derivatives (WH series) is shown in Scheme 1. Firstly resorcinol (**1**) reacted with 3-methyl-2-butenic acid (**2**) in the presence of zinc chloride in phosphorus oxychloride to afford 7-hydroxy-2,2-dimethylchroman-4-one (**3**). Reaction of **3** with dibromoethane provided 7-(2-bromoethoxy)-2,2-dimethylchroman-4-one (**4**), which was followed by substitution reaction with various alkylamines to give chromanone derivatives **WH1-WH6**. Amide **6** was efficiently synthesized from substituted aniline **5** in the presence of Et<sub>3</sub>N through an acylation reaction of chloroacetyl chloride, which was subsequently reacted with **3** to yield chromanone derivatives **WH7-WH10**.

<Insert Scheme 1>

The synthetic route of 2*H*-benzo[h]chromene-5-carboxylate **13** as key intermediate for the 2*H*-benzo[h]chromene derivatives is presented in Scheme 2. Salicylaldehyde (**7**) as starting material was reacted with benzyl chloride to afford benzyl protected product **8**. Stobbe condensation reaction of **8** with diethyl succinate gave condensed product **9**, and then further cyclization in acetic anhydride under reflux conditions produced 4-acetoxynaphthoate **10**. Subsequently, the acetyl group of **10** was deprotected with K<sub>2</sub>CO<sub>3</sub> in methanol, providing 4-hydroxynaphthoate **11**, which was then subjected to the [3+3] cycloaddition reaction with 3-methyl-2-butenal (**12**) to obtain a key intermediate **13**.

<Insert Scheme 2>

The synthetic routes of the 2*H*-benzo[h]chromene derivatives, encompassing the WI, WJ, WK and WL series, are outlined in Scheme 3. The key intermediate **13** was hydrolyzed with NaOH to afford 2*H*-benzo[h]chromene-5-carboxylic acid (**14**), which was then subjected to amidation reaction with corresponding amines in the presence of TBTU to give amide intermediates **15a-c**. Deprotection and double bond reduction of **14** and **15a-c** were carried out with hydrogen under the catalysis of Pd/C, providing hydroxyl intermediates **16a-d**, which were then reacted with corresponding substituted benzyl chloride (or bromide) to obtain 5-(2,6-dimethylmorpholinoyl)-2*H*-benzo[h]chromene derivatives

**W11-W19** and 5-(morpholinylalkyl)-2*H*-benzo[h]chromene derivatives **WL1-WL10**, respectively.

In addition, **13** was also treated with NaBH<sub>4</sub> in tetrahydrofuran (THF) to provide the corresponding alcohol **17**. Further bromination of **17** by CBr<sub>4</sub> and PPh<sub>3</sub> in dichloromethane produced brominated intermediate **18**, followed by a substitution reaction with 1,2,3,4-tetrazole and 2,6-dimethylmorpholine in DMF using potassium carbonate as a base to afford 1,2,3,4-tetrazolyl product **19a** and dimethylmorpholinyl product **19b**, respectively. Deprotection and double bond reduction of **19a** and **19b** and subsequent reaction with corresponding substituted benzyl chloride (or bromide) gave 5-(1,2,3,4-tetrazolylmethyl)-2*H*-benzo[h]chromene derivatives **WJ1-WJ10** and 5-(morpholinylalkyl)-2*H*-benzo[h]chromene derivatives **WL11-WL13**.

Furthermore, **13** was successfully converted to hydrazide **21** by hydrazinolysis, and subsequent treatment with triethyl orthoformate under reflux conditions generated 1,3,4-oxadiazole product **22**. Catalytic hydrogenation of **22** produced deprotected product **23**, which was transformed by treatment with the appropriate substituted benzyl halide to 5-(1,3,4-oxadiazolyl)-2*H*-benzo[h]chromene derivatives **WK1-WK9**.

<Insert **Scheme 3**>

### 2.3. Inherent antibacterial activity

The minimum inhibitory concentration (MIC) of all chromanone and 2*H*-benzo[h]chromene derivatives were initially determined using an antimicrobial susceptibility assay. This was necessary so that sub-inhibitory concentrations of the compounds could be investigated in subsequent checkerboard titration assays to measure efflux pump inhibition without a direct antibacterial effect. For this purpose, the MDR strain *E. coli* BW25113, expressing AcrB, was assayed alongside an isotypic strain with AcrB deleted. None of the target compounds showed any antibacterial activity against the wildtype strain at 512 µg/mL above tested strains, except **WK7** that was active at 64 µg/mL.

### 2.4 Ability to reverse bacterial resistance

The efflux pump inhibitory activity of all compounds was addressed by assaying their ability to reverse the resistance of certain antibiotics. All chromanone and 2*H*-benzo[h]chromene derivatives were tested in combination with known substrates of AcrB, namely erythromycin (ERY), chloramphenicol (CAM), tetraphenylphosphonium (TPP) and levofloxacin (LEV). Standard checkerboard assays in which the MIC values of a panel of antibiotics were determined in the presence of varying concentrations of the tested compounds were performed [33, 34, 36]. Known EPIs **NDGA** and **A3** served as reference compounds. Rifampicin (RIF) was also included as a negative control as this is not an AcrB substrate. Hence, any synergism with RIF would indicate the compound does not act specifically upon AcrB. Only those compounds that reduced the MIC values against wild type *E. coli* BW25113 expressing AcrB for at least one antimicrobial by 2-fold or more are presented in Table 1 and Table 2. Importantly, the absence of antibacterial activity at the high concentration of 512 µg/mL against *E. coli* BW25113 eliminated the possibility that the reversal of resistance in the checkerboard assays below was due to any intrinsic antibacterial activity of the compounds.

In the first stage of optimization, we focused on the modification of the aromatic moiety and linker of chromanone core to give the chromanone derivatives (WH series). In this series, only three compounds (**WH3**, **WH4** and **WH8**) displayed weak or moderate synergism with antibiotics (Table 1). Among them, **WH3** (8 µg/mL) and **WH4** (32 µg/mL) potentiated the activity of LEV by 2-fold, while **WH4** and **WH8** reduced the MIC values of TPP by 2- and 4-fold at

lower concentration than the reference molecules. Moreover, **WH8** at 64  $\mu\text{g}/\text{mL}$  increased bacterial sensitivity to CAM and TPP by 2- and 4-fold, respectively. However, none of compounds in this series showed synergism with ERY. Although a limited SARs was provided from the WH series chromanone derivatives, we could conclude that the chromanone core was not an optimal scaffold for AcrB inhibitory activity.

An alternative optimization strategy was carried out by substitution of the chromanone core with a large 2*H*-benzo[h]chromene core because the AcrB inhibition potency was particularly sensitive to the hydrophobic structure scaffold. On this basis, we introduced 2,6-dimethylmorpholinoyl and 1,2,3,4-tetrazolylmethylene groups (R section) at the C-5 position of the 2*H*-benzo[h]chromene core and varied the substituents on terminal benzene ring (R' section) at the C-7 position to obtain the 5-(2,6-dimethylmorpholinoyl)-2*H*-benzo[h]chromene derivatives (WI series) and the 5-(1,2,3,4-tetrazolylmethyl)-2*H*-benzo[h]chromene derivatives (WJ series), respectively. Those compounds that reduced the MIC by 2-fold or more in the WI and WJ series are listed in Table 1. Only **WI7** and **WI8** were moderately active with **WI7** increasing sensitivity towards Lev by 2-fold at 8  $\mu\text{g}/\text{ml}$  and **WI8** to both ERY and TPP at the highest concentration tested at 128  $\mu\text{g}/\text{mL}$ . In stark contrast, the WJ series exhibited improved antibacterial activity, with five compounds **WJ1**, **WJ5**, **WJ6**, **WJ7** and **WJ10** reversing resistance. Noteworthy were **WJ1**, **WJ5**, **WJ7** and **WJ10** that were active with two antibiotics in the testing panel. However, the WJ series showed a narrow antibacterial spectrum and weak synergism. The lack of biological activity in these two series was possibly due to the space constraint of the hydrophilic binding site between the 2*H*-benzo[h]chromene core and the resident water molecule. Bulky substituents, such as 2,6-dimethylmorpholinoyl and 1*H*-tetrazolylmethylene groups, may not be well accommodated by the hydrophilic cavity, resulting in the absence of necessary hydrogen bonding interactions mediated by water molecule.

<Insert Table 1>

Subsequently, we introduced small polar substituents (e.g. oxadiazolyl, morpholinylalkyl, carboxylic acid, and hydrazide) in the R positions, and investigated the effects of simultaneous changes of R and R' groups on the potentiating capacity of the compounds. These structural modifications led to the 5-(1,3,4-oxadiazolyl)-2*H*-benzo[h]chromene derivatives (WK) and the 5-(morpholinylalkyl)-2*H*-benzo[h]chromene derivatives (WL series). The data of antibacterial synergism of the WK and WL series are summarized in Table 2. Many compounds containing 1,3,4-oxadiazolyl or morpholinyl groups in the WK and WL series showed promising antibacterial synergism and broad-spectrum activity with certain exemplars yielding upto 16-fold reduction of the MIC values. Noteworthy were **WK2**, **WL1**, **WL7** and **WL10** that were broadly active against all antibacterials. Similarly, **WK1**, **WK5**, **WK7**, **WL2**, **WL7** and **WL9** were synergistic with three out of the four antibiotics in the screening panel. Moreover, all the active compounds were inhibitors of ERY efflux, with **WK2**, **WL7** and **WL10** displaying a desirable combination of potency and broad-spectrum activity. **WL1** increased bacterial sensitivity to CAM and TPP by 8- and 16-fold, showing greater potent synergistic activity than reference molecule. **WK2** was also an efficient resensitizer as it potentiated the antimicrobial activity of ERY, TPP and LEV by 2-fold at the low concentration of 8  $\mu\text{g}/\text{mL}$ , and synergized with all tested four antibacterials, leading upto a 16-fold MIC reduction at 128  $\mu\text{g}/\text{mL}$ . However, none of the compounds had effect on the MIC value of RIF (16  $\mu\text{g}/\text{mL}$ ) consistent with the hypothesis that these compounds acted as EPIs targeting AcrB.

The chromanone (WH series) and 2*H*-benzo[h]chromene derivatives (WI-WL series) contain three discrete structural fragments, which provided an opportunity to estimate an impact of each feature upon bioactivity. Considering the influence of the aromatic core fragments, the 2*H*-benzo[h]chromene core (WI-WL series) seem to be more profitable

than the chromanone core (WH series). For example, only three compounds possessing the chromanone core in the WH series (**WH3**, **WH4** and **WH8**) displayed weak or moderate synergism activity at high doses, while those compounds with the 2*H*-benzo[h]chromene core in the WJ-WL series, such as **WK1**, **WK2**, **WK5**, **WL1**, **WL7** and **WL10**, showed desirable potency and broad-spectrum activity at low concentrations. This highlights the 2*H*-benzo[h]chromene core as a promising scaffold for EPI activity. For the hydrophilic fragments (R groups) at the C-5 position of the 2*H*-benzo[h]chromene core, 1,3,4-oxadiazolyl and morpholinoyl substituents were optimal to improve the antibacterial effect of all four tested antibacterials, whereas 2,6-dimethylmorpholinoyl and 1,2,3,4-tetrazolylmethylene groups were disfavored. As exemplified by **WI1** and **WK2**, replacement of 2,6-dimethylmorpholinoyl group with 1,3,4-oxadiazolyl group resulted in a significant improved synergism activity, which imply that a small polar group for R is necessary for the activity. It is possible that the smaller polar groups can be well accommodated in the hydrophilic binding site and form additional hydrogen bonding interactions with water molecules. Thus, the most preferred substituents for EPI activity are as follows: morpholinoyl > 1,3,4-oxadiazolyl > carboxyl > 1,2,3,4-tetrazolylmethylene > 2,6-dimethylmorpholinoyl  $\approx$  2,6-dimethylmorpholinomethylene. Considering the influence of substitution at the benzene ring (R' groups) on the biological activities, it is noted that 4-methyl (**WK2**) and 4-acrylamido (**WL10**) groups were the most favorable. Furthermore, the substituent-free phenyl group (**WK1**, **WL1** and **WL7**) was more beneficial than the 3-methoxyphenyl group (**WK4**, **WL2** and **WL8**). In addition, a para-substituent on the benzene ring was favored as well. For instance, **WK3**, containing an *o*-methyl substituted phenyl group (**WK3** vs **WK2**), showed loss of EPI activity, possibly due to the absence of hydrophobic contacts in the para-position.

<Insert Table 2>

### 2.5. The effect of the compounds on substrate transport

The bioactive compounds in the checkerboard assays described above were then assayed to determine if they directly inhibited efflux mediated by AcrB in whole cell efflux assays [36, 37]. The lipophilic fluorescent dye Nile Red was employed as it is a known substrate of the AcrAB-TolC pump. Nile Red is weakly fluorescent in aqueous environments but undergoes a significant increase in fluorescence once inside the cell [7, 33]. Assays were performed upon *E. coli* BW255113 cells and an isogenic AcrB deletion used to help establish the specificity of AcrB-mediated substrate efflux and EPI mechanism of action. In this efflux assay, **WK5**, **WK7**, **WJ10**, **WL8** and **WL9** were identified as the most potent EPIs as they completely inhibited substrate efflux to the same level as the AcrB deletion strain at the low concentration of 50  $\mu$ M (Fig. 3). Similarly, **WH3**, **WI7**, **WI8**, **WJ1**, **WJ5**, **WJ6**, **WK1**, **WK2**, **WK3**, **WK6**, **WL1**, **WL2**, **WL7** and **WL10** also showed complete inhibitory activity at 100  $\mu$ M. In contrast, **WH4**, **WH8**, **WJ7** and **WK4** were weakly active, with inhibitory activity only observed at much higher concentrations of 100-200  $\mu$ M (**Fig. 1S** in Supporting data).

<Insert Fig. 3>

### 2.6. The effect of the compounds on the bacterial outer membrane

The outer membrane of Gram-negative bacteria is effective at limiting permeation of antibiotics into the cell. Compounds that permeabilise this barrier may allow the accumulation of antibiotics inside the cells and provide similar effects as EPIs [18, 35]. To determine if the active compounds described above possessed undesirable off-target membrane permeabilisation properties, a nitrocefin hydrolysis assay was performed on intact *E. coli* BW25513. Hydrolysis of the chromogenic  $\beta$ -lactam nitrocefin by  $\beta$ -lactamase produces a red compound that can be monitored by spectroscopy. The rapid hydrolysis of nitrocefin is indicative of a permeabilised outer membrane that facilitates increased diffusion of the reagent into the bacterial periplasm. The known membrane disruptor, polymyxin B (PMBN), served as a positive control. The results, shown in Fig. 4, demonstrated that none of the bioactive compounds in either the WH-WL series affected the permeability of the outer membrane at the tested concentrations, indicating their synergism with antibacterials was not due to membrane permeabilization.

<Insert Fig. 4>

### 2.7. The effect of the compounds on the bacterial inner membrane

Finally, chemical damage of the inner membrane and consequential perturbation of the proton motive force (pmf) that drives AcrAB-TolC activity was finally evaluated. As AcrB utilizes the pmf to transport substrates, those compounds that perturb the pmf across the inner membrane can also inhibit efflux by an indirect, off-target mechanism [38]. To determine whether the active compounds perturbed the pmf, we assessed the ability of those compounds to depolarize the bacterial transmembrane potential ( $\Delta\psi$ ) by using the membrane potential-sensitive dye 3,3-diethyloxycarbocyanine iodide (DiOC<sub>2</sub>(3)). DiOC<sub>2</sub>(3) undergoes a significant increase in fluorescence once the pmf is established by the addition of glucose. Following the treatment of cells with the ionophore and proton decoupler CCCP, the  $\Delta\psi$  was dissipated and the fluorescence intensity decreased to the level before glucose stimulation (blue curves representing bacteria not treated with active compound). If a compound disrupted the inner membrane, the fluorescence of DiOC<sub>2</sub>(3) was decreased due to the inability of cells to establish a proton gradient. The results are shown in Fig. 5. Importantly, none of the compounds disrupted the bacterial inner membrane, except **WL1**, at the low concentration of 32  $\mu\text{g/mL}$ .

<Insert Fig. 5>

### 2.8. In vitro cytotoxicity toward mammalian cells

A crucial parameter for developing antimicrobial agents is their selectivity for bacterial cells over mammalian cells. Mammalian cells (HepG2 cells) were used to evaluate the in vitro cytotoxic effect of the most potent compounds **WK2** and **WL7**. Paclitaxel was used as a positive control ( $\text{IC}_{50}$ =12.6 nM). As shown in **Table 3**, when treating with **WK2** and **WL7** at the concentration of 10  $\mu\text{M}$ , the cell viability rates toward HepG2 cells were 94% and 98%, respectively, while the cell inhibition rates were 87% and 66% at 100  $\mu\text{M}$ , respectively. The cytotoxicity results demonstrated that **WK2** and **WL7** possessed low cytotoxicity toward mammalian cells, which had a safety profile much better than paclitaxel.

<Insert **Table 3**>

### 2.9. Molecular docking

Molecular docking studies were next performed to predict the possible binding mode, to explain the SARs and to guide future structural optimisation experiments. The crystal structure of AcrB (PDB code: 5eno) served as the receptor protein, and **WK2** and **WL10** were selected as representative EPIs for molecular docking. As illustrated in Fig. 6a, **WK2** was well accommodated in the well-defined hydrophobic trap of AcrB. The *2H*-benzo[h]chromene core and phenyl groups were oriented parallel to the aromatic side chains of Phe628 and Phe178 respectively, resulting in extensive  $\pi$ - $\pi$  stacking interactions. The gemdimethyl group attached at the C-2 position of the *2H*-benzo[h]chromene core was encased by Try327 and Met573 through hydrophobic interactions. Moreover, the nitrogen atom of 1,3,4-oxadiazolyl group at the C-5 position of the *2H*-benzo[h]chromene core formed a hydrogen bond with a water molecule, which, in turn, bound to Gln176 by hydrogen bonds. The flexible methyl ether linker at the C-7 position of the *2H*-benzo[h]chromene core induced a conformational flexibility in the molecule that allowed optimal  $\pi$ -stacking interactions between the two aromatic rings and side chains of Phe628 and Phe178. Notably, **WL10** adopted similar binding mode to **WK2**, forming strong  $\pi$ - $\pi$  stacking interactions with Phe628 and Phe178, and hydrogen bond networks with Gln176 and water molecule. Additionally, a critical water molecule bound to the nitrogen atom of 4-acrylamide group was involved in a hydrogen bond network with Gln151, Ser155 and Ala286, effectively anchoring the EPI to these three amino acid residues (Fig. 6b). We propose that this extended hydrogen bonding network contributes to the potent bioactivity of the optimal WK and WL series.

<Insert **Fig. 6**>

Overall, on the basis of an integrated molecular design strategy and molecular modeling, fifty-one benzochromene and *2H*-benzo[h]chromene derivatives were designed, synthesized and evaluated for their EPI activity. Among them, twenty-three compounds (**Table 4**) were found to synergize with at least one antibacterial. Preliminary SARs derived from this study suggest: (1) the compounds containing the *2H*-benzo[h]chromene core were favorable for enhanced the EPI activity, whereas those containing the chromanone core were less active; (2) the efflux inhibitory activity was dependent upon substituents at the C-5 position of *2H*-benzo[h]chromene core with 1,3,4-oxadiazolyl and morpholinoyl groups preferred; (3) introduction of a hydrophilic or lipophilic group at the *para* position of the terminal benzene ring are important contributors for activity, and the introduction of methyl and acylamido groups were optimal. In comparison to the lead compounds **A3** and **NDGA**, the *2H*-benzo[h]chromene derivatives described here seemed to be more favorable as they displayed superior efficacy, and possessed significant and desirable EPI activity, indicating a successful outcome for this structure-guided drug design program. More importantly, the above SARs provides new insight into the discovery of novel AcrB inhibitors.

<Insert **Table 4**>

Noteworthy are compounds in the WK and WL series containing 1,3,4-oxadiazolyl and morpholinoyl groups at the C-5 position of the 2*H*-benzo[h]chromene core, respectively, that generally display better efficacy than the other compounds in the above two series as well as those in the WH, WI and WJ series, which is probably due to form an additional hydrogen bond networks, resulting in tighter binding with AcrB. In all five series, exemplars **WK2**, **WL1**, **WL7** and **WL10** all exhibited broad-spectrum, and high-efficiency, EPI activity. Especially, **WK2** was the most efficient potential EPI as it potentiated the activity of ERY, TPP and LEV even at the low concentration of 8 µg/mL, and synergized with all four antibacterials tested, leading upto a 16-fold MIC reduction at 128 µg/mL. Moreover, **WL1** had the greatest synergism with CAM and increased its sensitivity by 8-fold at 128 µg/mL, whereas **WK2**, **WL7** and **WL10** at 128 µg/mL markedly decreased the MIC values of ERY, TPP and LEV by 8-, 16- and 6-fold, respectively. In contrast, the compounds in the WH, WI and WJ series only showed a narrow antibacterial spectrum and weak synergism. Subsequently, twenty-four compounds with synergetic activity were selected to further assess their ability to inhibit Nile Red efflux and their effect on inner- and outer membrane permeabilisation. The results showed that all the active compounds inhibited AcrB-mediated substrate efflux at a reasonable concentration, and none of them permeabilised the inner and outer membrane, except **WL1** that was a strong disruptor of the inner membrane. Consequently, **WH3**, **WH4**, **WH8**, **WI8**, **WI9**, **WJ1**, **WJ5-WJ7**, **WJ10**, **WK1-WK7**, **WL2** and **WL7-WL10** were all identified as ideal AcrB inhibitors using the selection criteria described by Lomovskaya et al [1, 39].

### 3. Conclusions

This study illustrates the successful application of an integrated molecular design approach followed by chemical optimizations proposed by *in silico* analyses to confirm 2*H*-benzo[h]chromene nucleus as an optimal scaffold to obtain novel and potent AcrB inhibitors. Fifty-one compounds were designed, synthesized and evaluated for their EPI activity. Twenty-three compounds were identified as ideal AcrB inhibitors that synergized with at least one antibacterials tested, leading to 2- to 16-fold MIC reduction. They were also able to completely inhibit Nile red efflux at 50-200 µM, and targeted specifically on the AcrB. Among the above ideal EPIs, **WK2**, **WL7** and **WL10** exhibited the most broad-spectrum, and high-efficiency EPI activity. In conclusion, these newly 2*H*-benzo[h]chromene derivatives display potent biological activities as a novel class of antibacterial adjuvants and have potential for further development.

### 4. Experimental

#### 4.1. Chemistry

All reagents and chemicals were commercially available and used without further purification. All reactions were monitored by analytical thin-layer chromatography (TLC) using silica gel GF254 plates. Purification of crude products was carried out by flash column chromatography using silica gel 60 (particle size 0.040-0.063 mm). <sup>1</sup>H NMR and <sup>13</sup>C NMR spectra were recorded by using Bruker instrument at 600 and 100 MHz spectrometer with TMS as an internal standard. The following abbreviations are used to denote peak patterns in NMR spectra: singlet (s), doublet (d), triplet (t), multiplet (m), as well as doublet of doublets (dd). Low-resolution mass spectra (ESI-MS) data were recorded on an API 4000 instrument (Applied Biosystems, Connecticut, USA). The purity of all target compounds was performed on an Agilent 1200 Series HPLC system ((Agilent, Santa Clara County, USA) equipped with a diamonil C18 column (150 ×

4.6 mm, 5  $\mu$ m). HPLC conditions: solvent A = H<sub>2</sub>O, solvent B = CH<sub>3</sub>OH; flow rate = 1.0 mL/min. All tested compounds have a purity  $\geq$  95%.

#### 4.1.1. 7-Hydroxy-2,2-dimethylchroman-4-one (**3**)

A mixture of resorcinol **1** (10.00 g, 90.82 mmol), 3-methyl-2-butenic acid (**2**) (9.09 g, 90.82 mmol), zinc chloride (13.74 g, 136.22 mmol) and phosphorus oxychloride (139.24 g, 0.91 mol) was heated at 50 °C for 3 h. The reaction mixture was then poured into ice water (80 mL), and the resulting precipitate was filtered off. The residue was purified by silica column chromatography to afford **3** (10.27 g, 59%) as brown solid. mp 172-174 °C, ESI-MS *m/z* calcd for C<sub>11</sub>H<sub>13</sub>N<sub>3</sub> [M + H]<sup>+</sup> 193.1, found 193.4.

#### 4.1.2. 7-(2-Bromoethoxy)-2,2-dimethylchroman-4-one (**4**)

To a solution of **3** (5.00 g, 26.00 mmol) in acetonitrile (50 mL) were added K<sub>2</sub>CO<sub>3</sub> (7.19 g, 52.00 mmol) and dibromoethane (19.55 g, 104.00 mmol). The reaction mixture was heated at 75 °C for 8 h. The mixture was concentrated under reduced pressure and purified by flash column chromatography on silica gel to give yellow oil **4** (4.53 g, 58%). ESI-MS *m/z* calcd for C<sub>13</sub>H<sub>16</sub>BrO<sub>3</sub> [M + H]<sup>+</sup> 299.0, found 299.1.

#### 4.1.3. General methods for the preparation of the chromanone derivatives **WH1-WH6**

A solution of **4** (150 mg, 0.50 mmol) in DMF (10 mL), K<sub>2</sub>CO<sub>3</sub> (140 mg, 1.00 mmol) and corresponding alkylamine (0.75 mmol) were added. The solution was stirred at 78 °C for 6 h. Upon completion, the reaction mixture was poured in water (40 mL) and extracted with dichloromethane, washed with brine, and the solvent was removed under vacuum. The residue was purified by flash column chromatography (DCM/MeOH) to afford the desired compounds.

##### 4.1.3.1. 7-(2-(2,6-Dimethylmorpholino)ethoxy)-2,2-dimethylchroman-4-one (**WH1**)

Colorless oil, yield 45%, R<sub>f</sub> = 0.33 (petroleum ether/EtOAc = 30:1). HPLC purity 100.00% (A%/B% = 25:75, R<sub>t</sub> = 4.183 min). <sup>1</sup>H NMR (400 MHz, DMSO-*d*<sub>6</sub>)  $\delta$  7.57 (d, *J* = 8.7 Hz, 1H), 6.52 (dd, *J* = 8.8, 2.3 Hz, 1H), 6.43 (d, *J* = 2.4 Hz, 1H), 4.06 (t, *J* = 5.7 Hz, 2H), 3.46 (dtd, *J* = 12.3, 6.0, 2.0 Hz, 2H), 2.78–2.69 (m, 2H), 2.63 (s, 2H), 2.58 (t, *J* = 5.7 Hz, 2H), 1.68–1.58 (m, 2H), 1.31 (s, 6H), 0.96 (d, *J* = 6.3 Hz, 6H). <sup>13</sup>C NMR (100 MHz, CDCl<sub>3</sub>)  $\delta$  191.03, 165.30, 161.89, 128.26, 114.21, 109.59, 101.78, 79.60, 71.57 (2C), 66.03, 59.78 (2C), 56.89, 48.58, 26.71 (2C), 19.15 (2C). ESI-HRMS *m/z* calcd for C<sub>19</sub>H<sub>28</sub>NO<sub>4</sub> [M + H]<sup>+</sup> 334.2018, found 334.2014.

##### 4.1.3.2. 2,2-Dimethyl-7-(2-((3-morpholinopropyl)amino)ethoxy)chroman-4-one (**WH2**)

Colorless oil, yield 59%, R<sub>f</sub> = 0.27 (petroleum ether/EtOAc = 30:1). HPLC purity 98.30% (A%/B% = 15:85, R<sub>t</sub> = 4.619 min). <sup>1</sup>H NMR (400 MHz, DMSO-*d*<sub>6</sub>)  $\delta$  7.58 (d, *J* = 8.8 Hz, 1H), 6.52 (dd, *J* = 8.8, 2.3 Hz, 1H), 6.42 (d, *J* = 2.3 Hz, 1H), 4.01 (t, *J* = 5.5 Hz, 2H), 3.47 (t, *J* = 4.6 Hz, 4H), 2.81 (t, *J* = 5.4 Hz, 2H), 2.63 (s, 2H), 2.53 (t, *J* = 6.9 Hz, 2H), 2.23 (q, *J* = 7.4, 5.7 Hz, 6H), 1.50 (p, *J* = 6.9 Hz, 2H), 1.31 (s, 6H). <sup>13</sup>C NMR (100 MHz, CDCl<sub>3</sub>)  $\delta$  190.99, 165.28, 161.89, 128.26, 114.25, 109.47, 101.71, 79.60, 67.45, 66.93 (2C), 57.42, 53.75 (2C), 48.59, 48.54, 48.44, 26.68, 26.22 (2C). ESI-MS *m/z* calcd for C<sub>19</sub>H<sub>28</sub>NO<sub>4</sub> [M + H]<sup>+</sup> 334.2, found 334.3. ESI-HRMS *m/z* calcd for C<sub>20</sub>H<sub>31</sub>N<sub>2</sub>O<sub>4</sub> [M + H]<sup>+</sup> 363.2284, found 363.2287.

##### 4.1.3.3. 7-(2-(Isopropylamino)ethoxy)-2,2-dimethylchroman-4-one (**WH3**)

Colorless oil, yield 95%,  $R_f = 0.38$  (petroleum ether/EtOAc = 30:1). HPLC purity 96.50% (A%/B% = 15:85,  $R_t = 7.804$  min).  $^1\text{H}$  NMR (400 MHz, DMSO- $d_6$ )  $\delta$  7.58 (d,  $J = 8.7$  Hz, 1H), 6.53 (dd,  $J = 8.8, 2.4$  Hz, 1H), 6.41 (d,  $J = 2.4$  Hz, 1H), 3.98 (t,  $J = 5.7$  Hz, 2H), 2.78 (t,  $J = 5.7$  Hz, 2H), 2.72–2.66 (m, 1H), 2.64 (s, 2H), 1.32 (s, 6H), 0.92 (d,  $J = 6.2$  Hz, 6H).  $^{13}\text{C}$  NMR (100 MHz,  $\text{CDCl}_3$ )  $\delta$  191.07, 165.47, 161.90, 128.24, 114.21, 109.58, 101.73, 79.59, 68.01, 48.58 (2C), 46.04, 26.70 (2C), 22.86 (2C). ESI-HRMS  $m/z$  calcd for  $\text{C}_{16}\text{H}_{24}\text{NO}_3$  [ $\text{M} + \text{H}$ ] $^+$  278.1756, found 278.1757.

#### 4.1.3.4. 7-(2-(Cyclopentylamino)ethoxy)-2,2-dimethylchroman-4-one (WH4)

Brown oil, yield 85%,  $R_f = 0.37$  (petroleum ether/EtOAc = 30:1). HPLC purity 100.00% (A%/B% = 15:85,  $R_t = 10.628$  min).  $^1\text{H}$  NMR (400 MHz, DMSO- $d_6$ )  $\delta$  7.58 (d,  $J = 8.8$  Hz, 1H), 6.52 (dd,  $J = 8.8, 2.3$  Hz, 1H), 6.41 (d,  $J = 2.3$  Hz, 1H), 3.98 (t,  $J = 5.7$  Hz, 2H), 2.96 (p,  $J = 6.3$  Hz, 1H), 2.77 (t,  $J = 5.7$  Hz, 2H), 2.63 (s, 2H), 1.70–1.61 (m, 2H), 1.58–1.48 (m, 2H), 1.39 (qd,  $J = 7.5, 5.4, 2.6$  Hz, 2H), 1.31 (s, 6H), 1.21 (qt,  $J = 8.0, 6.0, 2.6$  Hz, 2H).  $^{13}\text{C}$  NMR (100 MHz,  $\text{CDCl}_3$ )  $\delta$  191.04, 165.48, 161.89, 128.21, 114.17, 109.57, 101.71, 79.56, 68.01, 59.67, 48.57, 47.27, 33.15 (2C), 26.69 (2C), 24.07 (2C). ESI-HRMS  $m/z$  calcd for  $\text{C}_{18}\text{H}_{26}\text{NO}_3$  [ $\text{M} + \text{H}$ ] $^+$  304.1912, found 304.1899.

#### 4.1.3.5. 7-(2-((Furan-2-ylmethyl)amino)ethoxy)-2,2-dimethylchroman-4-one (WH5)

Brown oil, yield 64%,  $R_f = 0.40$  (petroleum ether/EtOAc = 30:1). HPLC purity 95.28% (A%/B% = 15:85,  $R_t = 6.082$  min).  $^1\text{H}$  NMR (400 MHz, DMSO- $d_6$ )  $\delta$  7.57 (d,  $J = 8.8$  Hz, 1H), 7.49 (d,  $J = 1.8$  Hz, 1H), 6.52 (dd,  $J = 8.8, 2.4$  Hz, 1H), 6.41 (d,  $J = 2.3$  Hz, 1H), 6.31 (dd,  $J = 3.1, 1.9$  Hz, 1H), 6.18 (d,  $J = 3.1$  Hz, 1H), 3.99 (t,  $J = 5.6$  Hz, 2H), 3.66 (s, 2H), 2.78 (t,  $J = 5.6$  Hz, 2H), 2.43 (p,  $J = 1.8$  Hz, 2H), 1.31 (s, 6H).  $^{13}\text{C}$  NMR (100 MHz,  $\text{CDCl}_3$ )  $\delta$  191.05, 165.38, 161.89, 153.41, 142.00, 128.25, 114.24, 110.15, 109.55, 107.18, 101.72, 79.59, 67.74, 48.58, 47.60, 46.07, 26.70 (2C). ESI-HRMS  $m/z$  calcd for  $\text{C}_{18}\text{H}_{22}\text{NO}_4$  [ $\text{M} + \text{H}$ ] $^+$  316.1549, found 316.1530.

#### 4.1.3.6. 7-(2-((1H-Benzod[*d*]imidazol-2-yl)thio)ethoxy)-2,2-dimethylchroman-4-one (WH6)

White solid, yield 50%, mp 68–70 °C,  $R_f = 0.32$  (petroleum ether/EtOAc = 30:1). HPLC purity 98.78% (A%/B% = 15:85,  $R_t = 7.514$  min).  $^1\text{H}$  NMR (400 MHz, DMSO- $d_6$ )  $\delta$  8.26 – 8.19 (m, 1H), 8.12 (d,  $J = 6.2$  Hz, 2H), 8.00–7.93 (m, 1H), 7.62 (td,  $J = 6.2, 5.6, 3.4$  Hz, 2H), 7.46 (s, 1H), 7.40 (s, 1H), 4.57 (t,  $J = 5.4$  Hz, 2H), 3.99 (t,  $J = 5.3$  Hz, 2H), 2.50 (q,  $J = 1.9$  Hz, 6H).  $^{13}\text{C}$  NMR (100 MHz, DMSO)  $\delta$  190.80, 165.01, 161.97, 150.07, 144.05, 132.71, 128.09, 122.75, 122.13, 121.59, 117.82, 114.33, 110.82, 109.92, 102.44, 80.11, 67.29, 48.19, 30.20, 26.60 (2C). ESI-RHMS  $m/z$  calcd for  $\text{C}_{21}\text{H}_{22}\text{NO}_3\text{S}$  [ $\text{M} + \text{H}$ ] $^+$  369.1273, found 369.1262.

#### 4.1.4. General methods for the preparation of amide 6

To a solution of substituted aniline **5** (10.00 mmol) in DCM (20 mL) were added  $\text{Et}_3\text{N}$  (20.00 mmol), and chloroacetic chloride (12.00 mmol) was added at 0 °C slowly. The solvent was removed in vacuo and the crude residue was purified by flash column chromatography on silica gel to give amide **6**.

#### 4.1.5. General methods for the preparation of the chromanone derivatives WH7-WH10

The preparation method of **WH7-WH10** is similar to that of **WH1-WH6**.

##### 4.1.5.1. 2-((2,2-Dimethyl-4-oxochroman-7-yl)oxy)-*N*-(4-nitrophenyl)acetamide (WH7)

Yellow solid, yield 46%, mp 196-198 °C,  $R_f = 0.78$  (petroleum ether/EtOAc = 10:1). HPLC purity 95.11% (A%/B% = 15:85,  $R_t = 2.532$  min).  $^1\text{H}$  NMR (400 MHz, DMSO- $d_6$ )  $\delta$  10.75 (s, 1H), 8.25 (dd,  $J = 9.1, 4.5$  Hz, 2H), 7.90 (d,  $J = 8.8$  Hz, 2H), 7.70 (d,  $J = 8.7$  Hz, 1H), 6.70 (dd,  $J = 8.8, 2.4$  Hz, 1H), 6.54 (d,  $J = 2.4$  Hz, 1H), 4.89 (s, 2H), 2.73 (d,  $J = 6.0$  Hz, 2H), 1.39 (s, 6H).  $^{13}\text{C}$  NMR (100 MHz, DMSO)  $\delta$  190.82, 167.37, 164.59, 161.69, 144.96, 143.03, 128.14, 126.28, 125.45, 119.74, 115.76, 114.67, 109.84, 102.61, 80.23, 67.50, 48.18, 26.57 (2C). ESI-MS  $m/z$  calcd for  $\text{C}_{19}\text{H}_{19}\text{N}_2\text{O}_6$  [M + H] $^+$  371.1, found 371.3.

#### 4.1.5.2. *N*-(4-Cyano-3-(trifluoromethyl)phenyl)-2-((2,2-dimethyl-4-oxochroman-7-yl)oxy)acetamide (**WH8**)

White solid, yield 56%, mp 176-178 °C,  $R_f = 0.75$  (petroleum ether/EtOAc = 10:1). HPLC purity 99.72% (A%/B% = 15:85,  $R_t = 3.973$  min).  $^1\text{H}$  NMR (400 MHz, DMSO- $d_6$ )  $\delta$  10.87 (s, 1H), 8.31 (d,  $J = 1.9$  Hz, 1H), 8.13 (d,  $J = 8.6$  Hz, 1H), 8.07 (dd,  $J = 8.7, 1.9$  Hz, 1H), 7.69 (d,  $J = 8.8$  Hz, 1H), 6.70 (dd,  $J = 8.8, 2.3$  Hz, 1H), 6.55 (d,  $J = 2.3$  Hz, 1H), 4.89 (s, 2H), 2.72 (s, 2H), 1.38 (s, 6H).  $^{13}\text{C}$  NMR (100 MHz, DMSO)  $\delta$  190.81, 167.84, 164.46, 161.68, 143.40, 137.03, 132.35, 128.15, 124.22, 122.90, 121.50, 117.36, 116.13, 114.73, 109.82, 102.69, 80.23, 67.43, 48.18, 26.56 (2C). ESI-HRMS  $m/z$  calcd for  $\text{C}_{21}\text{H}_{18}\text{F}_3\text{N}_2\text{O}_4$  [M + H] $^+$  419.1218, found 419.1213.

#### 4.1.5.3. *N*-(3,4-Dicyanophenyl)-2-((2,2-dimethyl-4-oxochroman-7-yl)oxy)acetamide (**WH9**)

White solid, yield 67%, mp 212-214 °C,  $R_f = 0.75$  (petroleum ether/EtOAc = 10:1). HPLC purity 100.00% (A%/B% = 15:85,  $R_t = 5.073$  min).  $^1\text{H}$  NMR (400 MHz, DMSO- $d_6$ )  $\delta$  10.87 (s, 1H), 8.31 (d,  $J = 2.0$  Hz, 1H), 8.14–8.01 (m, 2H), 7.69 (d,  $J = 8.8$  Hz, 1H), 6.69 (dd,  $J = 8.8, 2.4$  Hz, 1H), 6.54 (d,  $J = 2.4$  Hz, 1H), 4.89 (s, 2H), 2.72 (s, 2H), 1.39 (s, 6H).  $^{13}\text{C}$  NMR (100 MHz, DMSO)  $\delta$  190.83, 167.83, 164.46, 161.68, 143.32, 135.61, 128.15, 123.94, 116.52, 115.99, 114.73, 110.26, 109.83, 108.81, 103.29, 102.70, 80.25, 67.43, 48.18, 26.58 (2C). ESI-HRMS  $m/z$  calcd for  $\text{C}_{21}\text{H}_{19}\text{N}_3\text{O}_5$  [M + H] $^+$  376.1297, found 393.1292.

#### 4.1.5.4. *N*-(3-Acetamido-4-fluorophenyl)-2-((2,2-dimethyl-4-oxochroman-7-yl)oxy)acetamide (**WH10**)

White solid, yield 68%, mp 190-192 °C,  $R_f = 0.40$  (petroleum ether/EtOAc = 8:1). HPLC purity 99.51% (A%/B% = 15:85,  $R_t = 1.835$  min).  $^1\text{H}$  NMR (400 MHz, DMSO- $d_6$ )  $\delta$  10.49 (s, 1H), 8.07 (p,  $J = 4.5$  Hz, 1H), 7.72–7.62 (m, 3H), 7.42 (dd,  $J = 8.5, 1.9$  Hz, 1H), 6.69 (dd,  $J = 8.7, 2.4$  Hz, 1H), 6.53 (d,  $J = 2.4$  Hz, 1H), 4.83 (s, 2H), 2.77 (d,  $J = 4.5$  Hz, 3H), 2.72 (s, 2H), 1.39 (s, 6H).  $^{13}\text{C}$  NMR (100 MHz, DMSO)  $\delta$  190.83, 167.05, 164.60, 163.87, 161.69, 161.05, 158.59, 142.26, 131.35, 128.14, 115.45, 114.66, 109.86, 106.99, 102.62, 80.24, 67.50, 48.18, 26.76, 26.58 (2C). ESI-HRMS  $m/z$  calcd for  $\text{C}_{21}\text{H}_{21}\text{FN}_2\text{O}_5$  [M + H] $^+$  401.1512, found 423.1512.

#### 4.1.6. 2-(Benzyloxy)benzaldehyde (**8**)

To a suspension of salicylaldehyde **7** (0.00 g, 81.88 mmol) in DMF (40 mL) was added benzyl chloride (15.55 g, 122.83 mmol) and  $\text{K}_2\text{CO}_3$  (22.63 g, 163.77 mmol), and the mixture was kept stirring at 70 °C for 6 h. After the completion of the reaction, water (30 mL) was added, extracted with EtOAc (3  $\times$  20 mL), washed with brine, and dried over anhydrous  $\text{Na}_2\text{SO}_4$ . The solvent was removed in *vacuo*. The residue was purified by column chromatography to furnish **8** as white solid (13.52g, 78%). mp 48-50 °C, ESI-MS  $m/z$  calcd for  $\text{C}_{14}\text{H}_{13}\text{O}_2$  [M + H] $^+$  213.1, found 213.3.

#### 4.1.7. (*E*)-4-(2-(Benzyloxy)phenyl)-3-(ethoxycarbonyl)but-3-enoic acid (**9**)

Sodium (2.25 g, 98.00 mmol) was dissolved in EtOH (100 mL), which was added portionwise to a stirred solution of **8** (13.00 g, 61.25 mmol) and diethyl succinate (13.87 g, 79.62 mmol) in EtOH (50 mL). The reaction mixture was then stirred and refluxed for 4 h. After the reaction finished, the resulting solution was concentrated in *vacuo*. The residue was poured into water (300 mL), extracted three times with EtOAc, washed with saturated brine and dried with anhydrous Na<sub>2</sub>SO<sub>4</sub>. The organic phase was concentrated and purified by silica flash chromatography to afford **9** as brown oil (15.72 g, 75%). ESI-MS *m/z* calcd for C<sub>20</sub>H<sub>21</sub>O<sub>5</sub> [M + H]<sup>+</sup> 341.1, found 341.3.

#### 4.1.8. Ethyl 4-acetoxy-8-(benzyloxy)-2-naphthoate (**10**)

The above product **9** (15.00 g, 44.07 mmol) and sodium acetate (3.62 g, 44.07 mmol) were dissolved in acetic anhydride (118.18 g, 881.38 mmol). The reaction mixture was refluxed for 6 h. Upon completion of the reaction, the solution was evaporated to dryness. Then water (300 mL) was added, and extracted with DCM (3 × 60 mL), washed with saturated Na<sub>2</sub>CO<sub>3</sub> and brine. The combined organic layers were concentrated to dryness under vacuum, and recrystallized from EtOAc and Et<sub>2</sub>O to afford **10** as light yellow solid (14.57 g, 91%). mp 96-98 °C, ESI-MS *m/z* calcd for C<sub>22</sub>H<sub>24</sub>NO<sub>5</sub> [M + NH<sub>4</sub>]<sup>+</sup> 382.1, found 382.4.

#### 4.1.9. Ethyl 8-(benzyloxy)-4-hydroxy-2-naphthoate (**11**)

To a solution of **10** (10.00 g, 27.40 mmol) in MeOH (100 mL) at room temperature was added K<sub>2</sub>CO<sub>3</sub> (5.70 g, 41.20 mmol) slowly. After stirring for 2 h, the reaction solution was concentrated to dryness under vacuum. Water (100 mL) was added, and then acidified with concentrated hydrochloric acid to pH = 6. The resulting precipitate was filtered off, and recrystallized from EtOAc and hexane to obtain **11** as a white solid (13.52 g, 78%). mp 181-183 °C, ESI-MS *m/z* calcd for C<sub>20</sub>H<sub>22</sub>NO<sub>4</sub> [M + NH<sub>4</sub>]<sup>+</sup> 340.1, found 340.4.

#### 4.1.10. Ethyl 7-(benzyloxy)-2,2-dimethyl-2H-benzo[h]chromene-5-carboxylate (**13**)

A mixture of **11** (5.00 g, 15.51 mmol), 3-methyl-2-butenal **12** (1.57 g, 18.61 mmol), PhB(OH)<sub>2</sub> (2.08 g, 17.06 mmol), and acetic acid (10 mL) in toluene (120 mL) was refluxed using Dean-Stark trap for 34 h. The resultant reaction solution was diluted with EtOAc (200 mL), and washed with saturated Na<sub>2</sub>CO<sub>3</sub> and brine in turn. The organic layer was dried, and evaporated in *vacuo*. The resultant residue was purified by silica column chromatography to give **13** as yellow solid (3.50 g, 58%). mp 100-102 °C, ESI-MS *m/z* calcd for C<sub>25</sub>H<sub>28</sub>NO<sub>4</sub> [M + NH<sub>4</sub>]<sup>+</sup> 406.2, found 406.5.

#### 4.1.11. 7-(Benzyloxy)-2,2-dimethyl-2H-benzo[h]chromene-5-carboxylic acid (**14**)

To a stirred suspension of NaOH (2.06 g, 51.50 mmol) in mixed solution (MeOH:H<sub>2</sub>O = 1:1, 40 mL) was added **13** (4.00 g, 10.30 mmol). The mixture was stirred at 70 °C for 6 h. After the reaction came to end, MeOH was removed in *vacuo*. The resultant mixture was acidified with concentrated hydrochloric acid to pH = 1, the resulting precipitate was filtered off, and dried to give **14** as yellow solid (3.56 g, 96%). mp 161-163 °C, ESI-MS *m/z* calcd for C<sub>22</sub>H<sub>22</sub>O<sub>6</sub> [M - H]<sup>-</sup> 359.1, found 359.3

#### 4.1.12. (7-(Benzyloxy)-2,2-dimethyl-2H-benzo[h]chromen-5-yl)(2,6-dimethylmorpholino)methanone (**15a**)

To a stirred suspension of **14** (3.50 g, 9.71 mmol) in CH<sub>3</sub>CN (50 mL) was added TBTU (3.12 g, 9.71 mmol). The mixture was stirred at rt. for 1 h and then 2,6-dimethylmorpholine (cis:tran = 1:1) and *N,N*-diisopropylethylamine (1.12 g, 9.71 mmol) were added. The mixture was still stirred at rt. for another 2 h. The resulting suspension was evaporated

under reduced pressure and the residue was treated with 1N HCl, 5% NaHCO<sub>3</sub> and saturated brine, and dried over anhydrous Na<sub>2</sub>SO<sub>4</sub>. The organic extracts were concentrated under reduced pressure, and was purified by column chromatography (petroleum ether/EtOAc) to afford **15a** as yellow solid (3.23g, 77%). mp 160-162 °C, ESI-MS m/z calcd for C<sub>29</sub>H<sub>32</sub>NO<sub>4</sub> [M + H]<sup>+</sup> 458.2, found 458.4.

#### 4.1.13. 7-(Benzyloxy)-2,2-dimethyl-2H-benzo[h]chromene-5-carbohydrazide (**15b**)

Compound **15b** was prepared according to the procedure depicted for **15a**. Yellow solid, ESI-MS m/z calcd for C<sub>23</sub>H<sub>23</sub>N<sub>2</sub>O<sub>3</sub> [M + H]<sup>+</sup> 375.2, found 375.3.

#### 4.1.14. (7-(Benzyloxy)-2,2-dimethyl-2H-benzo[h]chromen-5-yl)(morpholino)methanone (**15c**)

Compound **15c** was prepared according to the procedure depicted for **15a**. Yellow solid, ESI-MS m/z calcd for C<sub>27</sub>H<sub>28</sub>NO<sub>4</sub> [M + H]<sup>+</sup> 430.2, found 430.5.

#### 4.1.15.

#### (2,6-Dimethyltetrahydro-2H-pyran-4-yl)(7-hydroxy-2,2-dimethyl-3,4-dihydro-2H-benzo[h]chromen-5-yl)methanone (**16a**)

To a solution of **15a** (2.50 g, 5.47 mmol) in MeOH (20 mL) was added Pd/C (100 mg) under an atmosphere of hydrogen. The mixture was stirred overnight. The resulting solution was filtered off to remove palladium carbon. The filtrate was concentrated in vacuo to give **16a** (2.21g) as white solid, which was used for the next step without further purification. ESI-MS m/z calcd for C<sub>22</sub>H<sub>28</sub>NO<sub>4</sub> [M + H]<sup>+</sup> 370.2, found 370.5.

#### 4.1.16. 7-Hydroxy-2,2-dimethyl-3,4-dihydro-2H-benzo[h]chromene-5-carbohydrazide (**16b**)

Compound **16b** was prepared according to the procedure depicted for **16a**. white solid, ESI-MS m/z calcd for C<sub>16</sub>H<sub>19</sub>N<sub>2</sub>O<sub>3</sub> [M + H]<sup>+</sup> 287.1, found 287.3.

#### 4.1.17. (7-Hydroxy-2,2-dimethyl-3,4-dihydro-2H-benzo[h]chromen-5-yl)(morpholino)methanone (**16c**)

Compound **16c** was prepared according to the procedure depicted for **16a**. Yellow solid, ESI-MS m/z calcd for C<sub>20</sub>H<sub>24</sub>NO<sub>4</sub> [M + H]<sup>+</sup> 342.2, found 342.1.

#### 4.1.18. 7-Hydroxy-2,2-dimethyl-3,4-dihydro-2H-benzo[h]chromene-5-carboxylic acid (**16d**)

Compound **16d** was prepared according to the procedure depicted for **16a**. Yellow solid, ESI-MS m/z calcd for C<sub>16</sub>H<sub>15</sub>O<sub>4</sub> [M - H] 271.1, found 271.5.

#### 4.1.19. General procedure for the preparation of the 5-(2,6-dimethylmorpholinoyl)-2H-benzo[h]chromene derivatives **WI1-WI9**

To a solution of **15** (0.44 mmol, 1.0 eq) in CH<sub>3</sub>CN (20 mL) was slowly added K<sub>2</sub>CO<sub>3</sub> (0.88 mmol, 2.0 eq) and substituted benzyl halide (0.66 mmol, 1.5 eq). The reaction mixture was stirred at 55 °C for 4-8 h and concentrated in *vacuo*. The residue was redissolved in EtOAc (30 mL), washed with brine, dried with Na<sub>2</sub>SO<sub>4</sub> and concentrated. The residue was purified by silica gel column chromatography (petroleum ether/EtOAc) to yield the target compounds **WI1-WI 9** that were the mixture (*cis* : *tran* = 1:1).

## 4.1.19.1.

(2,2-Dimethyl-7-((4-methylbenzyl)oxy)-3,4-dihydro-2H-benzo[h]chromen-5-yl)(2,6-dimethyl-morpholino)methanone (**WI1**)

White solid, yield 73%, mp 212-214 °C,  $R_f = 0.74$  (petroleum ether/EtOAc = 10:1). HPLC purity 100.00% (A%/B% = 5:95,  $R_t = 3.749$  min).  $^1\text{H NMR}$  (600 MHz,  $\text{CDCl}_3$ )  $\delta$  7.83 (d,  $J = 8.5$  Hz, 1H), 7.70 (d, 1H), 7.45–7.37 (m, 3H), 7.25 (dd,  $J = 8.0, 3.0$  Hz, 2H), 6.92 (d,  $J = 7.6$  Hz, 1H), 5.26–5.16 (t, 2H), 4.70 (dd, 1H), 3.78–3.63 (m, 1H), 3.63–3.45 (m, 1H), 3.43–3.29 (m, 1H), 3.01 (ddt, 1H), 2.75 (ddd, 1H), 2.70–2.58 (m, 1H), 2.58–2.51 (m, 1H), 2.41 (s, 3H), 1.98–1.86 (m, 2H), 1.45 (d,  $J = 2.3$  Hz, 6H), 1.29 (dd,  $J = 6.4, 2.6$  Hz, 3H), 1.05 (d,  $J = 6.2$  Hz, 3H). ESI-HRMS  $m/z$  calcd for  $\text{C}_{30}\text{H}_{36}\text{NO}_4$  [M + H] $^+$  474.2644, found 474.2851.

## 4.1.19.2.

(7-((4-(Tert-butyl)benzyl)oxy)-2,2-dimethyl-3,4-dihydro-2H-benzo[h]chromen-5-yl)(2,6-dimethyl-morpholino)methanone (**WI2**)

White solid, yield 49%, mp 200-202 °C,  $R_f = 0.79$  (petroleum ether/EtOAc = 10:1). HPLC purity 95.61% (A%/B% = 5:95,  $R_t = 5.052$  min).  $^1\text{H NMR}$  (600 MHz,  $\text{CDCl}_3$ )  $\delta$  7.84 (d,  $J = 8.5$  Hz, 1H), 7.73 (d, 1H), 7.46 (t,  $J = 2.3$  Hz, 4H), 7.42–7.37 (m, 1H), 6.96 – 6.91 (m, 1H), 5.21 (t,  $J = 5.4$  Hz, 2H), 4.71 (dd, 1H), 3.79–3.64 (m, 1H), 3.64–3.46 (m, 1H), 3.36 (dd, 1H), 3.01 (ddt, 1H), 2.86–2.69 (m, 1H), 2.68–2.58 (m, 1H), 2.56 (d, 1H), 1.92 (m, 2H), 1.45 (d,  $J = 2.0$  Hz, 6H), 1.38 (s, 9H), 1.29 (t,  $J = 5.6$  Hz, 3H), 1.05 (dd,  $J = 6.5, 3.1$  Hz, 3H). ESI-HRMS  $m/z$  calcd for  $\text{C}_{33}\text{H}_{42}\text{NO}_4$  [M + H] $^+$  516.3114, found 516.3363.

## 4.1.19.3.

(2,6-Dimethylmorpholino)(7-((3-methoxybenzyl)oxy)-2,2-dimethyl-3,4-dihydro-2H-benzo[h]-chromen-5-yl)methanone (**WI3**)

White solid, yield 64%, mp 176-178 °C,  $R_f = 0.71$  (petroleum ether/EtOAc = 10:1). HPLC purity 95.04% (A%/B% = 5:95,  $R_t = 3.216$  min).  $^1\text{H NMR}$  (600 MHz,  $\text{CDCl}_3$ )  $\delta$  7.84 (d,  $J = 8.5$  Hz, 1H), 7.69 (s, 1H), 7.37 (dt, 2H), 7.10 (d,  $J = 7.6$  Hz, 1H), 7.05 (t,  $J = 1.9$  Hz, 1H), 6.93–6.88 (m, 2H), 5.22 (t,  $J = 5.2$  Hz, 2H), 4.71 (dd, 1H), 3.85 (s, 3H), 3.77–3.46 (m, 2H), 3.38 (dd, 1H), 3.02 (ddt, 1H), 2.77 (ddd, 1H), 2.69–2.52 (m, 2H), 1.94 (ddd, 2H), 1.45 (d,  $J = 2.6$  Hz, 6H), 1.30 (dd,  $J = 6.6, 3.1$  Hz, 3H), 1.05 (dd,  $J = 6.3, 3.8$  Hz, 3H). ESI-HRMS  $m/z$  calcd for  $\text{C}_{30}\text{H}_{36}\text{NO}_5$  [M + H] $^+$  490.2590, found 490.3004.

## 4.1.19.

4.4-(((5-(2,6-Dimethylmorpholine-4-carbonyl)-2,2-dimethyl-3,4-dihydro-2H-benzo[h]chromen-7-yl)oxy)methyl)benzonitrile (**WI4**)

White solid, yield 68%, mp 186-188 °C,  $R_f = 0.63$  (petroleum ether/EtOAc = 10:1). HPLC purity 98.94% (A%/B% = 5:95,  $R_t = 2.407$  min).  $^1\text{H NMR}$  (600 MHz,  $\text{CDCl}_3$ )  $\delta$  7.87 (d,  $J = 8.4$  Hz, 1H), 7.73 (d,  $J = 8.0$  Hz, 2H), 7.68 (d, 1H), 7.62 (d,  $J = 8.0$  Hz, 2H), 7.37 (t,  $J = 8.0$  Hz, 1H), 6.85 (d,  $J = 7.6$  Hz, 1H), 5.35–5.27 (m, 2H), 4.74–4.66 (m, 1H), 3.77–3.63 (m, 1H), 3.60–3.50 (m, 1H), 3.34 (dd, 1H), 3.01 (ddt, 1H), 2.85–2.70 (m, 1H), 2.70–2.60 (m, 1H), 2.57 (dq, 1H), 1.93 (dt, 2H), 1.45 (s, 6H), 1.30 (dd,  $J = 6.3, 3.1$  Hz, 3H), 1.05 (t,  $J = 6.1$  Hz, 3H). ESI-RHMS  $m/z$  calcd for  $\text{C}_{30}\text{H}_{32}\text{N}_2\text{O}_4$  [M + H] $^+$  485.2440, found 485.2796.

## 4.1.19.5.

(2,6-Dimethylmorpholino)(7-((4-fluorobenzyl)oxy)-2,2-dimethyl-3,4-dihydro-2H-benzo[h]-chromen-5-yl)-methanone (WI5)

White solid, yield 75%, mp 194-196 °C,  $R_f = 0.67$  (petroleum ether/EtOAc = 10:1). HPLC purity 99.68% (A%/B% = 5:95,  $R_t = 9.416$  min).  $^1\text{H NMR}$  (600 MHz,  $\text{CDCl}_3$ )  $\delta$  7.85 (d,  $J = 8.4$  Hz, 1H), 7.68 (d, 1H), 7.48 (t,  $J = 6.6$  Hz, 2H), 7.42–7.36 (m, 1H), 7.13 (t,  $J = 8.3$  Hz, 2H), 6.91 (d,  $J = 2.7$  Hz, 1H), 5.20 (t,  $J = 4.6$  Hz, 2H), 4.70 (dd, 1H), 3.70 (dt, 1H), 3.60–3.48 (m, 1H), 3.35 (dd, 1H), 3.01 (ddt, 1H), 2.76 (dt, 1H), 2.69–2.53 (m, 2H), 1.94 (qd, 2H), 1.45 (s, 6H), 1.29 (t,  $J = 5.3$  Hz, 3H), 1.05 (t,  $J = 5.4$  Hz, 3H). ESI-MS  $m/z$  calcd for  $\text{C}_{29}\text{H}_{33}\text{FNO}_4$   $[\text{M} + \text{H}]^+$  478.2, found 478.5.

## 4.1.19.6.

(7-((2,4-Dichlorobenzyl)oxy)-2,2-dimethyl-3,4-dihydro-2H-benzo[h]chromen-5-yl)(2,6-dimethyl-morpholino)methanone (WI6)

White solid, yield 68%, mp 92-94 °C,  $R_f = 0.64$  (petroleum ether/EtOAc = 10:1). HPLC purity 98.31% (A%/B% = 5:95,  $R_t = 8.184$  min).  $^1\text{H NMR}$  (600 MHz,  $\text{CDCl}_3$ )  $\delta$  7.86 (d,  $J = 8.5$  Hz, 1H), 7.69 (d, 1H), 7.56 (d,  $J = 8.3$  Hz, 1H), 7.47 (t,  $J = 1.4$  Hz, 1H), 7.39 (t,  $J = 8.1$  Hz, 1H), 7.32 (dd,  $J = 8.3, 2.0$  Hz, 1H), 6.88 (d,  $J = 7.6$  Hz, 1H), 5.30 (d,  $J = 1.8$  Hz, 2H), 4.76–4.67 (m, 1H), 3.78–3.63 (m, 1H), 3.62–3.50 (m, 1H), 3.37 (ddt, 1H), 3.02 (ddt, 1H), 2.78 (ddd, 1H), 2.69–2.60 (m, 1H), 2.60–2.52 (m, 1H), 1.99–1.86 (m, 2H), 1.45 (d,  $J = 2.2$  Hz, 6H), 1.30 (dd,  $J = 6.3, 2.7$  Hz, 3H), 1.05 (t,  $J = 5.9$  Hz, 3H). ESI-HRMS  $m/z$  calcd for  $\text{C}_{29}\text{H}_{32}\text{Cl}_2\text{NO}_4$   $[\text{M} + \text{H}]^+$  528.1708, found 528.1889.

## 4.1.19.7.

(7-((2,6-Dichlorobenzyl)oxy)-2,2-dimethyl-3,4-dihydro-2H-benzo[h]chromen-5-yl)(2,6-dimethyl-morpholino)methanone (WI7)

White solid, yield 45%, mp 112-114 °C,  $R_f = 0.68$  (petroleum ether/EtOAc = 10:1). HPLC purity 97.57% (A%/B% = 5:95,  $R_t = 3.824$  min).  $^1\text{H NMR}$  (600 MHz,  $\text{CDCl}_3$ )  $\delta$  7.90–7.84 (m, 1H), 7.63–7.53 (m, 1H), 7.47–7.38 (m, 3H), 7.31 (dd,  $J = 8.6, 7.6$  Hz, 1H), 7.06 (dd,  $J = 7.7, 0.9$  Hz, 1H), 5.58–5.36 (m, 2H), 4.67 (dd, 1H), 3.66 (s, 1H), 3.50 (d, 1H), 3.37 (dd, 1H), 3.16–2.88 (m, 1H), 2.82–2.50 (m, 3H), 1.91 (dt, 2H), 1.47–1.43 (m, 6H), 1.27 (dd,  $J = 7.1, 4.2$  Hz, 3H), 1.10–1.01 (m, 3H). ESI-HRMS  $m/z$  calcd for  $\text{C}_{29}\text{H}_{32}\text{Cl}_2\text{NO}_4$   $[\text{M} + \text{H}]^+$  528.1708, found 528.1939.

## 4.1.19.8.

(7-((4-Bromobenzyl)oxy)-2,2-dimethyl-3,4-dihydro-2H-benzo[h]chromen-5-yl)(2,6-dimethyl-morpholino)methanone (WI8)

White solid, yield 54%, mp 198-199 °C,  $R_f = 0.64$  (petroleum ether/EtOAc = 10:1). HPLC purity 97.71% (A%/B% = 5:95,  $R_t = 3.694$  min).  $^1\text{H NMR}$  (600 MHz,  $\text{CDCl}_3$ )  $\delta$  7.85 (d,  $J = 8.5$  Hz, 1H), 7.67 (d, 1H), 7.55 (d,  $J = 8.3$  Hz, 2H), 7.42–7.36 (m, 3H), 6.87 (d,  $J = 7.6$  Hz, 1H), 5.19 (d,  $J = 5.8$  Hz, 2H), 4.71 (dd, 1H), 3.68 (dd, 1H), 3.62–3.46 (m, 1H), 3.36 (dd, 1H), 3.14–2.90 (m, 1H), 2.86–2.70 (m, 1H), 2.70–2.53 (m, 2H), 1.92 (h,  $J = 7.7$  Hz, 2H), 1.45 (s, 6H), 1.30 (d,  $J = 6.3$  Hz, 3H), 1.05 (d,  $J = 6.3$  Hz, 3H). ESI-HRMS  $m/z$  calcd for  $\text{C}_{29}\text{H}_{33}\text{BrNO}_4$   $[\text{M} + \text{H}]^+$  538.1593, found 538.1797.

## 4.1.19.9.

(2,2-Dimethyl-7-((4-nitrobenzyl)oxy)-3,4-dihydro-2H-benzo[h]chromen-5-yl)(2,6-dimethyl-morpholino)methanone (WI9)

Yellow solid, yield 71%, mp 182-184 °C,  $R_f$  = 0.62 (petroleum ether/EtOAc = 10:1). HPLC purity 98.19% (A%/B% = 10:90,  $R_t$  = 3.694 min).  $^1\text{H}$  NMR (600 MHz,  $\text{CDCl}_3$ )  $\delta$  8.30 (d,  $J$  = 8.6 Hz, 2H), 7.88 (d,  $J$  = 8.4 Hz, 1H), 7.74–7.63 (m, 3H), 7.37 (t,  $J$  = 8.1 Hz, 1H), 6.86 (d,  $J$  = 7.6 Hz, 1H), 5.36 (s, 2H), 4.71 (dd, 1H), 3.77–3.63 (m, 1H), 3.61–3.48 (m, 1H), 3.36 (dd, 1H), 3.01 (ddt, 1H), 2.85–2.70 (m, 1H), 2.70–2.53 (m, 2H), 1.94 (qd, 2H), 1.46 (s, 6H), 1.30 (d,  $J$  = 6.1 Hz, 3H), 1.05 (t,  $J$  = 5.1 Hz, 3H). ESI-HRMS  $m/z$  calcd for  $\text{C}_{29}\text{H}_{33}\text{N}_2\text{O}_6$   $[\text{M} + \text{H}]^+$  505.2338, found 505.2597.

#### 4.1.20. General procedure for the preparation of the 5-(morpholinylalkyl)-2H-benzo[h]chromene derivatives **WL1-WL10**

The preparation method of **WL1-WL10** is similar to that of **WI1-WI9**.

##### 4.1.20.1. 7-(Benzyloxy)-2,2-dimethyl-3,4-dihydro-2H-benzo[h]chromene-5-carboxylic acid (**WL1**)

White solid, yield 87%, mp 189-191 °C,  $R_f$  = 0.29 (petroleum ether/EtOAc = 5:1). HPLC purity 97.88% (A%/B% = 25:75,  $R_t$  = 1.603 min).  $^1\text{H}$  NMR (600 MHz,  $\text{CDCl}_3$ )  $\delta$  8.76 (d,  $J$  = 0.9 Hz, 1H), 7.86 (dt,  $J$  = 8.5, 0.9 Hz, 1H), 7.57–7.53 (m, 2H), 7.48–7.43 (m, 3H), 7.39–7.36 (m, 1H), 6.93–6.90 (m, 1H), 5.31 (s, 2H), 3.29 (t,  $J$  = 6.8 Hz, 2H), 1.93 (t,  $J$  = 6.8 Hz, 2H), 1.47 (s, 6H).  $^{13}\text{C}$  NMR (150 MHz,  $\text{CDCl}_3$ )  $\delta$  173.01, 155.14, 149.41, 136.94, 129.20, 128.66 (2C), 127.96, 127.92, 127.29 (2C), 125.84, 123.93, 119.10, 115.39, 114.34, 106.01, 74.29, 70.19, 32.73, 26.73 (2C), 21.81. ESI-HRMS  $m/z$  calcd for  $\text{C}_{23}\text{H}_{26}\text{NO}_4$   $[\text{M} - \text{H}]^-$  361.1440, found 361.1437.

##### 4.1.20.2. 7-((3-Methoxybenzyl)oxy)-2,2-dimethyl-3,4-dihydro-2H-benzo[h]chromene-5-carboxylic acid (**WL2**)

White solid, yield 76%, mp 184-186 °C,  $R_f$  = 0.26 (petroleum ether/EtOAc = 5:1). HPLC purity 99.36% (A%/B% = 15:85,  $R_t$  = 1.606 min).  $^1\text{H}$  NMR (600 MHz,  $\text{CDCl}_3$ )  $\delta$  8.79 (d,  $J$  = 0.8 Hz, 1H), 7.86 (d,  $J$  = 8.5 Hz, 1H), 7.49–7.43 (m, 1H), 7.36 (t,  $J$  = 7.8 Hz, 1H), 7.14–7.10 (m, 2H), 6.94–6.89 (m, 2H), 5.29 (s, 2H), 3.87 (s, 3H), 3.30 (t,  $J$  = 6.8 Hz, 2H), 1.94 (t,  $J$  = 6.8 Hz, 2H), 1.47 (s, 6H).  $^{13}\text{C}$  NMR (150 MHz,  $\text{CDCl}_3$ )  $\delta$  173.25, 159.88, 155.11, 149.42, 138.59, 129.69, 129.22, 128.00, 125.82, 123.94, 119.38, 119.19, 115.43, 114.39, 113.71, 112.39, 106.09, 74.29, 70.09, 55.26, 32.73, 26.73 (2C), 21.82. ESI-HRMS  $m/z$  calcd for  $\text{C}_{24}\text{H}_{27}\text{NO}_5$   $[\text{M} - \text{H}]^-$  391.1546, found 391.1544.

##### 4.1.20.3. 7-((4-Acetamidobenzyl)oxy)-2,2-dimethyl-3,4-dihydro-2H-benzo[h]chromene-5-carboxylic acid (**WL3**)

White solid, yield 77%, mp 150-152 °C,  $R_f$  = 0.41 (petroleum ether/EtOAc = 10:1). HPLC purity 95.28% (A%/B% = 10:90,  $R_t$  = 3.501 min).  $^1\text{H}$  NMR (400 MHz,  $\text{DMSO}-d_6$ )  $\delta$  10.21 (s, 1H), 9.78 (s, 1H), 8.29 (s, 1H), 7.39 (d,  $J$  = 8.2 Hz, 2H), 7.08 (d,  $J$  = 7.8 Hz, 1H), 6.80 (t,  $J$  = 7.4 Hz, 3H), 4.51 (s, 2H), 3.01 (t,  $J$  = 6.8 Hz, 2H), 1.98 (s, 3H), 1.67 (t,  $J$  = 6.8 Hz, 2H), 0.97 (s, 6H).  $^{13}\text{C}$  NMR (100 MHz,  $\text{DMSO}-d_6$ )  $\delta$  169.30, 168.36, 153.15, 151.03, 138.80, 136.97, 132.71, 128.13 (2C), 127.92, 127.44, 125.64, 124.71, 119.06 (2C), 117.76, 115.17, 108.76, 74.26, 41.89, 32.12, 26.04 (2C), 24.38, 21.81. ESI-HRMS  $m/z$  calcd for  $\text{C}_{25}\text{H}_{29}\text{N}_2\text{O}_5$   $[\text{M} - \text{H}]^-$  418.1655, found 418.1650.

##### 4.1.20.4. 7-(Benzyloxy)-2,2-dimethyl-3,4-dihydro-2H-benzo[h]chromene-5-carbohydrazide (**WL4**)

White solid, yield 32%. mp 170-172 °C,  $R_f$  = 0.48 (petroleum ether/EtOAc = 10:1). HPLC purity 98.56% (A%/B% = 12:88,  $R_t$  = 2.534 min).  $^1\text{H}$  NMR (600 MHz,  $\text{CDCl}_3$ )  $\delta$  7.89 (s, 1H), 7.85–7.82 (m, 1H), 7.51 (dd,  $J$  = 7.3, 1.8 Hz, 2H), 7.47–7.42 (m, 2H), 7.43–7.37 (m, 2H), 7.28 (s, 1H), 6.91 (d,  $J$  = 7.7 Hz, 1H), 5.24 (s, 2H), 4.23–4.11 (s, 2H), 3.01 (t,  $J$  = 6.7 Hz, 2H), 1.88 (t,  $J$  = 6.7 Hz, 2H), 1.45 (s, 6H).  $^{13}\text{C}$  NMR (150 MHz,  $\text{CDCl}_3$ )  $\delta$  170.72, 154.52, 149.48, 136.84, 131.75, 128.68 (2C), 128.09, 127.78, 127.57 (2C), 126.62, 124.16, 114.41, 113.14, 112.38, 106.01, 74.68, 70.31, 32.47, 26.87 (2C), 20.62. ESI-MS  $m/z$  calcd for  $\text{C}_{23}\text{H}_{25}\text{N}_2\text{O}_3$   $[\text{M} + \text{H}]^+$  377.2, found 377.4.

4.1.20.5. 7-((3-Methoxybenzyl)oxy)-2,2-dimethyl-3,4-dihydro-2H-benzo[h]chromene-5-carbohydrazide (**WL5**)

White solid, yield 73%, mp 139-141 °C,  $R_f = 0.38$  (petroleum ether/EtOAc = 10:1). HPLC purity 99.58% (A%/B% = 18:82,  $R_t = 3.244$  min).  $^1\text{H}$  NMR (600 MHz,  $\text{CDCl}_3$ )  $\delta$  7.91–7.88 (m, 1H), 7.83 (d,  $J = 8.5$  Hz, 1H), 7.43–7.32 (m, 3H), 7.09 (dd,  $J = 7.7, 1.3$  Hz, 1H), 7.05 (t,  $J = 2.0$  Hz, 1H), 6.93–6.87 (m, 2H), 5.21 (s, 2H), 4.02 (d, 2H), 3.84 (s, 3H), 3.00 (t,  $J = 6.7$  Hz, 2H), 1.87 (t,  $J = 6.7$  Hz, 2H), 1.44 (s, 6H).  $^{13}\text{C}$  NMR (150 MHz,  $\text{CDCl}_3$ )  $\delta$  170.70, 159.84, 154.49, 149.47, 138.44, 131.70, 129.75, 127.78, 126.61, 124.15, 119.75, 114.43, 113.37, 113.21, 113.16, 112.43, 106.06, 74.68, 70.22, 55.28, 32.46, 26.86 (2C), 20.62. ESI-MS  $m/z$  calcd for  $\text{C}_{24}\text{H}_{27}\text{N}_2\text{O}_4$   $[\text{M} + \text{H}]^+$  407.2, found 407.4.

4.1.20.6.

*N*-(4-(((5-(Hydrazinecarbonyl)-2,2-dimethyl-3,4-dihydro-2H-benzo[h]chromen-7-yl)oxy)methyl)phenyl)acetamide (**WL6**)

White solid, yield 53%, mp 225-227 °C,  $R_f = 0.27$  (petroleum ether/EtOAc = 5:1). HPLC purity 97.38% (A%/B% = 30:70,  $R_t = 8.856$  min).  $^1\text{H}$  NMR (600 MHz,  $\text{DMSO}-d_6$ )  $\delta$  10.04 (s, 1H), 9.77 (s, 1H), 9.49 (s, 1H), 7.70 (s, 1H), 7.39 (d,  $J = 8.3$  Hz, 2H), 7.03 (d,  $J = 7.8$  Hz, 1H), 6.79 (d,  $J = 8.0$  Hz, 3H), 4.51 (s, 2H), 4.47 (s, 2H), 2.78 (t,  $J = 6.9$  Hz, 2H), 1.99 (s, 3H), 1.66 (t,  $J = 6.8$  Hz, 2H), 0.98 (s, 6H).  $^{13}\text{C}$  NMR (150 MHz,  $\text{DMSO}-d_6$ )  $\delta$  168.96, 168.36, 152.65, 150.64, 138.98, 136.92, 133.36, 131.37, 128.10 (2C), 126.22, 125.56, 125.16, 119.07 (2C), 113.57, 113.43, 108.56, 74.47, 41.93, 31.95, 26.14 (2C), 24.38, 20.77. ESI-MS: calcd for  $\text{C}_{25}\text{H}_{31}\text{N}_4\text{O}_4$   $[\text{M} + \text{NH}_4]^+$  451.2, found 451.4.

4.1.20.7. (7-(Benzyloxy)-2,2-dimethyl-3,4-dihydro-2H-benzo[h]chromen-5-yl)(morpholino)methanone (**WL7**)

White solid, yield 85%, mp 171-172 °C,  $R_f = 0.70$  (petroleum ether/EtOAc = 10:1). HPLC purity 100.00% (A%/B% = 15:85,  $R_t = 6.633$  min).  $^1\text{H}$  NMR (400 MHz,  $\text{DMSO}-d_6$ )  $\delta$  7.66 (d,  $J = 8.4$  Hz, 1H), 7.52 (d,  $J = 7.1$  Hz, 2H), 7.48 (s, 1H), 7.45 – 7.33 (m, 4H), 7.08 (d,  $J = 7.7$  Hz, 1H), 5.29 (s, 2H), 3.67 (s, 4H), 3.48 (s, 2H), 3.18 (d,  $J = 5.7$  Hz, 2H), 2.70 (d, 2H), 1.88 (s, 2H), 1.38 (s, 6H).  $^{13}\text{C}$  NMR (100 MHz,  $\text{CDCl}_3$ )  $\delta$  169.92, 154.45, 149.38, 137.00, 133.17, 128.62 (2C), 127.99, 127.42 (2C), 126.88, 125.86, 124.82, 114.31, 111.56, 110.79, 106.00, 74.70, 70.19, 66.97 (2C), 47.46, 41.97, 32.33, 26.93, 26.76, 20.21. ESI-HRMS  $m/z$  calcd for  $\text{C}_{27}\text{H}_{30}\text{NO}_4$   $[\text{M} + \text{H}]^+$  432.2175, found 432.2135.

4.1.20.8. (7-((3-Methoxybenzyl)oxy)-2,2-dimethyl-3,4-dihydro-2H-benzo[h]chromen-5-yl)(morpholino)methanone (**WL8**)

White solid, yield 64%, mp 138-140 °C,  $R_f = 0.68$  (petroleum ether/EtOAc = 10:1). HPLC purity 96.10% (A%/B% = 15:85,  $R_t = 5.142$  min).  $^1\text{H}$  NMR (600 MHz,  $\text{CDCl}_3$ )  $\delta$  7.83 (d,  $J = 8.5$  Hz, 1H), 7.73 (s, 1H), 7.36 (dt,  $J = 12.8, 7.9$  Hz, 2H), 7.10 (d,  $J = 7.5$  Hz, 1H), 7.05 (t,  $J = 2.0$  Hz, 1H), 6.94–6.88 (m, 2H), 5.22 (d,  $J = 4.1$  Hz, 2H), 3.93 – 3.86 (m, 2H), 3.85 (s, 3H), 3.84–3.77 (m, 2H), 3.60 (d,  $J = 33.7$  Hz, 2H), 3.34 (d,  $J = 45.6$  Hz, 2H), 3.10 – 3.00 (m, 1H), 2.63 (d,  $J = 17.1$  Hz, 1H), 1.93 (q,  $J = 8.4, 7.4$  Hz, 2H), 1.45 (s, 6H).  $^{13}\text{C}$  NMR (150 MHz,  $\text{CDCl}_3$ )  $\delta$  169.89, 159.83, 154.44, 149.39, 138.62, 133.17, 129.69, 126.88, 125.86, 124.82, 119.63, 114.34, 113.36, 113.00, 111.59, 110.82, 106.07, 74.70, 70.15, 66.98, 55.28, 47.48, 41.98, 32.34, 26.94, 26.72, 20.22. ESI-MS  $m/z$  calcd for  $\text{C}_{28}\text{H}_{32}\text{NO}_5$   $[\text{M} + \text{H}]^+$  462.2, found 462.4.

4.1.20.9.

(2,2-Dimethyl-7-((4-(trifluoromethyl)benzyl)oxy)-3,4-dihydro-2H-benzo[h]chromen-5-yl)(morpholino)methanone (**WL9**)

White solid, yield 44%, mp 242-244 °C,  $R_f$  = 0.62 (petroleum ether/EtOAc = 10:1). HPLC purity 100.00% (A%/B% = 15:85,  $R_t$  = 5.555 min).  $^1\text{H}$  NMR (600 MHz,  $\text{CDCl}_3$ )  $\delta$  7.86 (d,  $J$  = 8.5 Hz, 1H), 7.73–7.67 (m, 3H), 7.63 (d,  $J$  = 8.0 Hz, 2H), 7.37 (t,  $J$  = 8.1 Hz, 1H), 6.87 (d,  $J$  = 7.6 Hz, 1H), 5.30 (s, 2H), 3.89 (q,  $J$  = 5.1 Hz, 2H), 3.86–3.79 (m, 2H), 3.66–3.53 (m, 2H), 3.41–3.26 (m, 2H), 3.04 (dt,  $J$  = 15.3, 6.8 Hz, 1H), 2.70–2.59 (m, 1H), 1.94 (q,  $J$  = 7.1 Hz, 2H), 1.46 (s, 6H).  $^{13}\text{C}$  NMR (150 MHz,  $\text{CDCl}_3$ )  $\delta$  169.84, 153.99, 149.47, 141.04, 133.49, 127.34 (2C), 126.92, 125.75, 125.64, 125.62, 125.59, 125.57, 124.99, 124.73, 114.74, 111.70, 110.47, 106.02, 74.79, 69.31, 66.97, 47.45, 41.98, 32.30, 26.87, 26.77, 20.21. ESI-MS  $m/z$  calcd for  $\text{C}_{28}\text{H}_{29}\text{F}_3\text{NO}_4$  [M + H] $^+$  500.2, found 500.3.

#### 4.1.20.10.

#### *N*-(4-(((2,2-Dimethyl-5-(morpholine-4-carbonyl)-3,4-dihydro-2H-benzo[*h*]chromen-7-yl)oxy)methyl)phenyl)acrylamide (**WL10**)

White solid, yield 38%, mp 128-130 °C,  $R_f$  = 0.27 (petroleum ether/EtOAc = 10:1). HPLC purity 98.82% (A%/B% = 15:85,  $R_t$  = 3.294 min).  $^1\text{H}$  NMR (600 MHz,  $\text{DMSO-}d_6$ )  $\delta$  10.22 (s, 1H), 7.72 (d,  $J$  = 8.4 Hz, 2H), 7.66 (d,  $J$  = 8.5 Hz, 1H), 7.50–7.45 (m, 3H), 7.39 (t,  $J$  = 8.1 Hz, 1H), 7.09 (d,  $J$  = 7.7 Hz, 1H), 6.45 (dd,  $J$  = 17.0, 10.1 Hz, 1H), 6.28 (dd,  $J$  = 17.0, 1.9 Hz, 1H), 5.78–5.75 (m, 1H), 5.23 (s, 2H), 3.69 (d,  $J$  = 19.8 Hz, 4H), 3.54–3.42 (m, 2H), 3.19 (d,  $J$  = 13.3 Hz, 2H), 2.83–2.55 (m, 2H), 1.87 (q,  $J$  = 6.6 Hz, 2H), 1.38 (s, 6H).  $^{13}\text{C}$  NMR (150 MHz,  $\text{DMSO-}d_6$ )  $\delta$  168.65, 163.62, 154.27, 149.02, 139.24, 134.39, 132.38, 132.29, 128.90 (2C), 127.42, 126.47, 126.31, 124.50, 119.80 (2C), 114.03, 112.30, 110.09, 107.02, 75.15, 69.87, 66.73, 55.38, 47.37, 41.84, 31.99, 27.02, 26.81, 20.04. ESI-HRMS  $m/z$  calcd for  $\text{C}_{30}\text{H}_{33}\text{N}_2\text{O}_5$  [M - H] $^-$  499.2233, found 499.2243.

#### 4.1.21. (7-(Benzyloxy)-2,2-dimethyl-2H-benzo[*h*]chromen-5-yl)methanol (**17**)

The key intermediate **13** (3.00 g, 7.72 mmol) was dissolved in THF (20 mL) at 0 °C.  $\text{LiAlH}_4$  (0.59 g, 15.44 mmol) was slowly added to the above solution. The mixture was stirred for another 2 h. After the reaction completed, the mixture was quenched with water (30 mL), extracted with DCM (3  $\times$  35 mL), washed with saturated brine, dried with sodium sulphate and concentrated *in vacuo*. The residue was purified via silica gel column chromatography (petroleum ether/EtOAc) to give **17** as yellow solid (2.07 g, 77%). mp 96-98 °C, ESI-MS  $m/z$  calcd for  $\text{C}_{23}\text{H}_{26}\text{NO}_3$  [M +  $\text{NH}_4$ ] $^+$  364.2, found 364.4.

#### 4.1.22. 7-(Benzyloxy)-5-(bromomethyl)-2,2-dimethyl-2H-benzo[*h*]chromene (**18**)

To a solution of **17** (2.00 g, 5.77 mmol) and  $\text{CBr}_4$  (2.11 g, 6.35 mmol) in DCM (15 mL) at 0 °C was added  $\text{PPh}_3$  (1.67 g, 6.35 mmol) slowly. The mixture was stirred for 3 h, and the reaction solvents were concentrated to dryness. The residue was purified by flash column chromatography to afford **18** as yellow solid (1.63 g, 69%). mp 89-91 °C, ESI-MS  $m/z$  calcd for  $\text{C}_{23}\text{H}_{22}\text{BrO}_2$  [M + H] $^+$  409.1, found 409.4.

#### 4.1.23. 1-((7-(Benzyloxy)-2,2-dimethyl-2H-benzo[*h*]chromen-5-yl)methyl)-1H-tetrazole (**19a**)

A solution of **18** (3.80 g, 9.28 mmol),  $\text{K}_2\text{CO}_3$  (2.57 g, 18.56 mmol) and 1H-tetrazole (0.78 g, 11.14 mmol) in DMF (15 mL) was heated at 75 °C for 5 h. The reaction mixture was then cooled to room temperature, diluted with EtOAc (30 mL), and washed with water (30 mL). The organic extract was dried, and the residue was purified by flash column chromatography (petroleum ether/EtOAc) to afford **19a** as white solid (2.22 g, 47%). mp 100-102 °C, ESI-MS  $m/z$  calcd for  $\text{C}_{24}\text{H}_{24}\text{N}_5\text{O}_2$  [M +  $\text{NH}_4$ ] $^+$  416.2, found 416.5.

4.1.24. (2*S*,6*R*)-4-((7-(Benzyloxy)-2,2-dimethyl-2*H*-benzo[*h*]chromen-5-yl)methyl)-2,6-dimethyl-morpholine (**19b**)

Compound **19b** was prepared according to the procedure depicted for **19a**. Colorless oil, ESI-MS  $m/z$  calcd for  $C_{29}H_{34}NO_3$   $[M + H]^+$  444.2, found 444.5.

4.1.25. 5-((1*H*-Tetrazol-1-yl)methyl)-2,2-dimethyl-2*H*-benzo[*h*]chromen-7-ol (**20a**)

Compound **20a** was prepared according to the procedure depicted for **16a**. White solid, ESI-MS  $m/z$  calcd for  $C_{17}H_{22}N_5O_2$   $[M + NH_4]^+$  328.1, found 328.4.

4.1.26. 5-(((2*S*,6*R*)-2,6-Dimethylmorpholino)methyl)-2,2-dimethyl-2*H*-benzo[*h*]chromen-7-ol (**20b**)

Compound **20b** was prepared according to the procedure depicted for **16a**. Yellow solid, ESI-MS  $m/z$  calcd for  $C_{22}H_{30}NO_3$   $[M + H]^+$  356.2, found 356.4.

4.1.27. General procedure for the preparation of the 5-(1,2,3,4-tetrazolylmethyl)-2*H*-benzo[*h*]chromene derivatives **WJ1-WJ10**

The preparation method of **WJ1-WJ10** was similar to that of **WL1-WL10**.

4.1.27.1. 1-((7-(Benzyloxy)-2,2-dimethyl-3,4-dihydro-2*H*-benzo[*h*]chromen-5-yl)methyl)-1*H*-tetrazole (**WJ1**)

White solid, yield 71%, mp 145-147 °C,  $R_f$  = 0.52 (petroleum ether/EtOAc = 10:1). HPLC purity 97.61% (A%/B% = 10:90,  $R_t$  = 2.887 min).  $^1H$  NMR (400 MHz,  $CDCl_3$ )  $\delta$  8.48 (s, 1H), 7.87 (s, 1H), 7.79 (d,  $J$  = 8.4 Hz, 1H), 7.49 (d,  $J$  = 7.1 Hz, 2H), 7.45-7.39 (m, 2H), 7.39-7.31 (m, 2H), 6.86 (d,  $J$  = 7.7 Hz, 1H), 5.92 (s, 2H), 5.22 (s, 2H), 2.78 (t,  $J$  = 6.7 Hz, 2H), 1.89 (t,  $J$  = 6.7 Hz, 2H), 1.37 (s, 6H).  $^{13}C$  NMR (100 MHz,  $CDCl_3$ )  $\delta$  154.36, 152.96, 149.52, 137.07, 128.82, 128.60 (2C), 127.92, 127.34 (2C), 127.24, 125.98, 124.81, 115.57, 114.36, 113.82, 105.99, 74.18, 70.18, 55.44, 32.38, 26.67 (2C), 19.86. ESI-HRMS  $m/z$  calcd for  $C_{24}H_{28}N_5O_2$   $[M + H]^+$  401.1899, found 418.1864.

4.1.27.2. 1-((7-((3-Methoxybenzyl)oxy)-2,2-dimethyl-3,4-dihydro-2*H*-benzo[*h*]chromen-5-yl)methyl)-1*H*-tetrazole (**WJ2**)

White solid, yield 58%, mp 159-161 °C,  $R_f$  = 0.56 (petroleum ether/EtOAc = 8:1). HPLC purity 97.66% (A%/B% = 18:82,  $R_t$  = 6.277 min).  $^1H$  NMR (400 MHz,  $CDCl_3$ )  $\delta$  8.34 (s, 1H), 7.86 (s, 1H), 7.82 (d,  $J$  = 8.5 Hz, 1H), 7.40 (t,  $J$  = 8.1 Hz, 1H), 7.34 (t,  $J$  = 7.9 Hz, 1H), 7.09-7.01 (m, 2H), 6.91 (dd,  $J$  = 10.4, 7.0 Hz, 2H), 5.68 (s, 2H), 5.21 (s, 2H), 3.82 (s, 3H), 2.56 (t,  $J$  = 6.7 Hz, 2H), 1.85 (d,  $J$  = 13.4 Hz, 2H), 1.36 (s, 6H).  $^{13}C$  NMR (100 MHz,  $CDCl_3$ )  $\delta$  159.88, 154.26, 150.10, 142.25, 138.43, 129.77, 128.11, 127.46, 126.46, 124.80, 119.70, 115.64, 114.51, 113.37, 113.32, 113.27, 106.38, 74.44, 70.29, 55.30, 51.31, 32.15, 26.64 (2C), 19.63. ESI-HRMS  $m/z$  calcd for  $C_{25}H_{27}N_4O_3$   $[M + H]^+$  431.2083, found 431.1884.

4.1.27.3. 4-(((5-((1*H*-Tetrazol-1-yl)methyl)-2,2-dimethyl-3,4-dihydro-2*H*-benzo[*h*]chromen-7-yl)oxy)-methyl)benzotrile (**WJ3**)

White solid, yield 70%, mp 200-202°C,  $R_f$  = 0.50 (petroleum ether/EtOAc = 8:1). HPLC purity 97.07% (A%/B% = 18:82,  $R_t$  = 5.070 min).  $^1H$  NMR (400 MHz,  $CDCl_3$ )  $\delta$  8.51 (s, 1H), 7.82 (d,  $J$  = 8.5 Hz, 1H), 7.80 (s, 1H), 7.74-7.69 (m, 2H), 7.59 (d,  $J$  = 8.0 Hz, 2H), 7.33 (t,  $J$  = 8.1 Hz, 1H), 6.79 (d,  $J$  = 7.7 Hz, 1H), 5.95 (s, 2H), 5.28 (s, 2H), 2.82 (t,  $J$  = 6.7 Hz, 2H), 1.91 (t,  $J$  = 6.7 Hz, 2H), 1.39 (s, 6H).  $^{13}C$  NMR (100 MHz,  $CDCl_3$ )  $\delta$  153.66, 153.00, 149.63, 142.47, 132.48 (2C),

129.26, 127.49 (2C), 125.78, 124.63, 118.69, 115.00, 114.90, 113.99, 111.79, 106.00, 104.99, 74.31, 69.12, 55.29, 32.33, 26.66 (2C), 19.88. ESI-HRMS  $m/z$  calcd for  $C_{25}H_{27}N_6O_2$   $[M + H]^+$  426.1930, found 426.1918.

#### 4.1.27.4.

*1-((2,2-Dimethyl-7-((4-(trifluoromethyl)benzyl)oxy)-3,4-dihydro-2H-benzo[h]chromen-5-yl)methyl)-1H-tetrazole (WJ4)*  
 White solid, yield 65%, mp 158-160°C,  $R_f = 0.47$  (petroleum ether/EtOAc = 8:1). HPLC purity 98.52% (A%/B% = 10:90,  $R_t = 4.300$  min).  $^1H$  NMR (400 MHz,  $CDCl_3$ )  $\delta$  8.50 (s, 1H), 7.83 (s, 1H), 7.81 (d,  $J = 8.5$  Hz, 1H), 7.68 (d,  $J = 8.1$  Hz, 2H), 7.60 (d,  $J = 8.0$  Hz, 2H), 7.34 (t,  $J = 8.1$  Hz, 1H), 6.82 (d,  $J = 7.7$  Hz, 1H), 5.94 (s, 2H), 5.28 (s, 2H), 2.81 (t,  $J = 6.7$  Hz, 2H), 1.90 (t,  $J = 6.7$  Hz, 2H), 1.38 (s, 6H).  $^{13}C$  NMR (100 MHz,  $CDCl_3$ )  $\delta$  153.90, 152.99, 149.60, 141.11, 129.12, 127.29 (2C), 127.25, 125.86, 125.65, 125.61, 125.58, 125.54, 124.69, 115.16, 114.80, 113.95, 105.99, 74.27, 69.33, 55.34, 32.35, 26.66 (2C), 19.88. ESI-HRMS  $m/z$  calcd for  $C_{25}H_{27}F_3N_5O_2$   $[M + H]^+$  469.1851, found 469.1870.

#### 4.1.27.5.

*1-((2,2-Dimethyl-7-((4-(trifluoromethoxy)benzyl)oxy)-3,4-dihydro-2H-benzo[h]chromen-5-yl)methyl)-1H-tetrazole (WJ5)*

White solid, yield 46%, mp 154-156 °C,  $R_f = 0.57$  (petroleum ether/EtOAc = 8:1). HPLC purity 97.66% (A%/B% = 10:90,  $R_t = 3.538$  min).  $^1H$  NMR (400 MHz,  $CDCl_3$ )  $\delta$  8.36 (s, 1H), 7.84 (d,  $J = 8.5$  Hz, 1H), 7.79 (s, 1H), 7.51 (d,  $J = 8.5$  Hz, 2H), 7.40 (t,  $J = 8.1$  Hz, 1H), 7.28 (d,  $J = 8.1$  Hz, 2H), 6.90 (d,  $J = 7.7$  Hz, 1H), 5.70 (s, 2H), 5.23 (s, 2H), 2.58 (t,  $J = 6.7$  Hz, 2H), 1.86 (t,  $J = 6.6$  Hz, 2H), 1.37 (s, 6H).  $^{13}C$  NMR (100 MHz,  $CDCl_3$ )  $\delta$  153.97, 150.14, 148.98, 142.29, 135.51, 129.03, 128.84 (2C), 128.34, 127.45, 126.36, 124.70, 121.20 (2C), 115.21, 114.77, 113.43, 106.24, 74.49, 69.39, 51.24, 32.14, 26.63 (2C), 19.64. ESI-HRMS  $m/z$  calcd for  $C_{25}H_{23}F_3N_4O_3Na$   $[M + H]^+$  485.1800, found 485.1768.

#### 4.1.27.6. *1-((2,2-Dimethyl-7-((4-nitrobenzyl)oxy)-3,4-dihydro-2H-benzo[h]chromen-5-yl)methyl)-1H-tetrazole (WJ6)*

Yellow solid, yield 89%, mp 150-151 °C,  $R_f = 0.49$  (petroleum ether/EtOAc = 8:1). HPLC purity 97.63% (A%/B% = 10:90,  $R_t = 3.375$  min).  $^1H$  NMR (400 MHz,  $CDCl_3$ )  $\delta$  8.52 (s, 1H), 8.31–8.24 (m, 2H), 7.87–7.78 (m, 2H), 7.65 (d,  $J = 8.4$  Hz, 2H), 7.33 (t,  $J = 8.1$  Hz, 1H), 6.80 (d,  $J = 7.6$  Hz, 1H), 5.95 (s, 2H), 5.33 (s, 2H), 2.82 (t,  $J = 6.7$  Hz, 2H), 1.91 (t,  $J = 6.7$  Hz, 2H), 1.39 (s, 6H).  $^{13}C$  NMR (100 MHz,  $CDCl_3$ )  $\delta$  153.60, 153.02, 149.64, 147.64, 144.45, 129.32, 127.55 (2C), 127.26, 125.77, 124.63, 123.91 (2C), 115.09, 114.88, 114.03, 106.02, 74.33, 68.91, 55.28, 32.33, 26.66 (2C), 19.89. ESI-MS: calcd for  $C_{24}H_{27}N_6O_4$   $[M + NH_4]^+$  463.2, found 463.5.

#### 4.1.27.7.

*4-(((5-((1H-Tetrazol-1-yl)methyl)-2,2-dimethyl-3,4-dihydro-2H-benzo[h]chromen-7-yl)oxy)-methyl)-N-methylbenzamide (WJ7)*

White solid, yield 27%, mp 212-214 °C,  $R_f = 0.49$  (petroleum ether/EtOAc = 5:1). HPLC purity 97.34% (A%/B% = 10:90,  $R_t = 3.207$  min).  $^1H$  NMR (400 MHz,  $CDCl_3$ )  $\delta$  8.39 (s, 1H), 7.82 (dd,  $J = 10.1, 8.2$  Hz, 3H), 7.74 (s, 1H), 7.51 (d,  $J = 8.0$  Hz, 2H), 7.39 (t,  $J = 8.1$  Hz, 1H), 6.88 (d,  $J = 7.7$  Hz, 1H), 6.33–6.24 (m, 1H), 5.70 (s, 2H), 5.26 (s, 2H), 3.03 (d,  $J = 4.7$  Hz, 3H), 2.61 (t,  $J = 6.7$  Hz, 2H), 1.87 (t,  $J = 6.7$  Hz, 2H), 1.37 (s, 6H).  $^{13}C$  NMR (100 MHz,  $CDCl_3$ )  $\delta$  167.83, 153.96, 150.09, 142.36, 140.24, 134.44, 128.44, 127.38, 127.32 (2C), 127.26 (2C), 126.33, 124.77, 114.89, 114.77, 113.30, 106.49, 74.47, 69.79, 51.09, 32.15, 26.87, 26.63 (2C), 19.66. ESI-HRMS  $m/z$  calcd for  $C_{26}H_{28}N_5O_3$   $[M + H]^+$  458.2222, found 458.2434.

## 4.1.27.8.

4-(((5-((1*H*-Tetrazol-1-yl)methyl)-2,2-dimethyl-3,4-dihydro-2*H*-benzo[*h*]chromen-7-yl)oxy)methyl)-*N*-isopropylbenzamide (**WJ8**)

White solid, yield 59%, mp 201-203 °C,  $R_f$  = 0.45 (petroleum ether/EtOAc = 8:1). HPLC purity 99.85% (A%/B% = 25:75,  $R_t$  = 4.149min).  $^1\text{H}$  NMR (400 MHz, DMSO- $d_6$ )  $\delta$  9.55 (s, 1H), 8.36 (d,  $J$  = 7.6 Hz, 1H), 7.92–7.89 (m, 2H), 7.69 (d,  $J$  = 8.0 Hz, 2H), 7.49 (d,  $J$  = 8.0 Hz, 2H), 7.42 (s, 1H), 7.16 (d,  $J$  = 8.0 Hz, 1H), 5.89 (s, 2H), 5.31 (s, 2H), 4.06 (d,  $J$  = 6.9 Hz, 1H), 2.69 (t,  $J$  = 7.0 Hz, 2H), 1.71 (t,  $J$  = 6.9 Hz, 2H), 1.18 (d,  $J$  = 6.6 Hz, 6H), 0.94 (s, 6H).  $^{13}\text{C}$  NMR (100 MHz, DMSO- $d_6$ )  $\delta$  165.64, 152.71, 150.99, 147.24, 144.99, 140.48, 134.69, 132.00, 130.64, 127.94 (2C), 127.70, 127.35, 126.99 (2C), 125.40, 115.22, 106.52, 74.51, 69.25, 49.58, 41.45, 31.67, 25.92 (2C), 22.84 (2C), 19.71. ESI-MS  $m/z$  calcd for  $\text{C}_{28}\text{H}_{32}\text{N}_5\text{O}_3$  [M + H] $^+$  486.2, found 486.5.

4.1.27.9. *N*-(4-(((5-((1*H*-Tetrazol-1-yl)methyl)-2,2-dimethyl-3,4-dihydro-2*H*-benzo[*h*]chromen-7-yl)oxy)methyl)phenyl)acetamide (**WJ9**)

White solid, yield 39%, mp 195-197 °C,  $R_f$  = 0.38 (petroleum ether/EtOAc = 8:1). HPLC purity 96.28% (A%/B% = 10:90,  $R_t$  = 4.070 min).  $^1\text{H}$  NMR (400 MHz,  $\text{CDCl}_3$ )  $\delta$  8.36 (s, 1H), 7.82 (d,  $J$  = 8.6 Hz, 1H), 7.77 (s, 1H), 7.55 (d,  $J$  = 8.0 Hz, 2H), 7.47–7.35 (m, 4H), 6.91 (d,  $J$  = 7.7 Hz, 1H), 5.68 (s, 2H), 5.17 (s, 2H), 2.58 (t,  $J$  = 6.5 Hz, 2H), 2.18 (s, 3H), 1.85 (t,  $J$  = 6.6 Hz, 2H), 1.36 (s, 6H).  $^{13}\text{C}$  NMR (100 MHz,  $\text{CDCl}_3$ )  $\delta$  168.40, 154.23, 150.06, 142.32, 137.82, 132.61, 128.42 (2C), 128.19, 127.40, 126.42, 124.82, 120.10 (2C), 115.37, 114.51, 113.30, 106.42, 74.43, 70.08, 51.19, 32.15, 26.63 (2C), 24.59, 19.63. ESI-MS  $m/z$  calcd for  $\text{C}_{26}\text{H}_{28}\text{N}_5\text{O}_3$  [M + H] $^+$  458.2, found 458.5.

4.1.27.10. *N*-(4-(((5-((1*H*-Tetrazol-1-yl)methyl)-2,2-dimethyl-3,4-dihydro-2*H*-benzo[*h*]chromen-7-yl)oxy)methyl)phenyl)acrylamide (**WJ10**)

43%, mp 197-199 °C,  $R_f$  = 0.37 (petroleum ether/EtOAc = 8:1). HPLC purity 95.55% (A%/B% = 10:90,  $R_t$  = 6.173 min).  $^1\text{H}$  NMR (400 MHz,  $\text{CDCl}_3$ )  $\delta$  8.38 (s, 1H), 7.81 (d,  $J$  = 8.5 Hz, 2H), 7.75 (s, 1H), 7.64 (d,  $J$  = 8.0 Hz, 2H), 7.44–7.36 (m, 3H), 6.90 (d,  $J$  = 7.7 Hz, 1H), 6.49–6.39 (m, 1H), 6.30 (dd,  $J$  = 16.8, 10.1 Hz, 1H), 5.76 (d,  $J$  = 10.2 Hz, 1H), 5.66 (s, 2H), 5.15 (s, 2H), 2.58 (t,  $J$  = 6.6 Hz, 2H), 1.85 (t,  $J$  = 6.6 Hz, 2H), 1.36 (s, 6H).  $^{13}\text{C}$  NMR (100 MHz,  $\text{CDCl}_3$ )  $\delta$  163.73, 154.20, 150.03, 142.40, 137.74, 132.82, 131.14, 128.40 (2C), 128.26, 127.92, 127.37, 126.41 (2C), 124.79, 120.26, 115.26, 114.50, 113.29, 106.37, 74.42, 70.02, 51.15, 32.15, 26.63 (2C), 19.63. ESI-MS  $m/z$  calcd for  $\text{C}_{27}\text{H}_{28}\text{N}_5\text{O}_3$  [M + H] $^+$  470.2, found 470.4.

4.1.28. General procedure for the preparation of the 5-(morpholinylalkyl)-2*H*-benzo[*h*]chromene derivatives **WL11-WL13**

The preparation method of **WL11-WL13** was similar to that of **WL1-WL10**.

## 4.1.28.1.

(2*S*,6*R*)-4-((7-(Benzyloxy)-2,2-dimethyl-3,4-dihydro-2*H*-benzo[*h*]chromen-5-yl)methyl)-2,6-dimethylmorpholine (**WL11**)

White solid, yield 55%, mp 132-134 °C,  $R_f$  = 0.61 (petroleum ether/EtOAc = 10:1),  $[\alpha]_D^{25}$  = -153.85 (C=1,  $\text{CH}_3\text{OH}$ ). HPLC purity 96.23% (A%/B% = 2:98,  $R_t$  = 4.665 min).  $^1\text{H}$  NMR (400 MHz, DMSO- $d_6$ )  $\delta$  7.62 (d,  $J$  = 7.6 Hz, 2H), 7.53 (d,  $J$  = 7.0 Hz, 2H), 7.42 (t,  $J$  = 7.2 Hz, 2H), 7.38–7.33 (m, 1H), 7.30 (t,  $J$  = 8.1 Hz, 1H), 7.00 (d,  $J$  = 7.7 Hz, 1H), 5.29 (s,

2H), 3.53 (s, 4H), 2.92 (t,  $J = 6.8$  Hz, 2H), 2.69 (d,  $J = 10.8$  Hz, 2H), 1.85 (t,  $J = 6.7$  Hz, 2H), 1.70 (t,  $J = 10.6$  Hz, 2H), 1.35 (s, 6H), 1.03 (d,  $J = 6.2$  Hz, 6H).  $^{13}\text{C}$  NMR (100 MHz,  $\text{CDCl}_3$ )  $\delta$  154.16, 148.81, 137.45, 134.07, 128.55 (2C), 127.82, 127.24 (2C), 126.34, 124.63, 124.51, 115.75, 114.37, 114.21, 105.56, 73.85, 71.96 (2C), 70.12, 61.78, 59.52 (2C), 32.73, 26.81 (2C), 19.59, 19.17 (2C). ESI-MS  $m/z$  calcd for  $\text{C}_{29}\text{H}_{36}\text{NO}_3$   $[\text{M} + \text{H}]^+$  446.3, found 446.5.

#### 4.1.28.2.

(2*S*,6*R*)-4-((7-((3-Methoxybenzyl)oxy)-2,2-dimethyl-3,4-dihydro-2*H*-benzo[*h*]chromen-5-yl)methyl)-2,6-dimethylmorpholine (**WL12**)

White solid, yield 67%, mp 96-98 °C,  $R_f = 0.63$  (petroleum ether/EtOAc = 10:1),  $[\alpha]_D^{25} = -19.40$  (C=1,  $\text{CH}_3\text{OH}$ ). HPLC purity 99.05% (A%/B% = 2:98,  $R_t = 10.171$  min).  $^1\text{H}$  NMR (400 MHz,  $\text{DMSO}-d_6$ )  $\delta$  7.62 (t,  $J = 4.2$  Hz, 2H), 7.31 (dt,  $J = 12.9, 7.9$  Hz, 2H), 7.12–7.06 (m, 2H), 6.98 (d,  $J = 7.7$  Hz, 1H), 6.94–6.88 (m, 1H), 5.26 (s, 2H), 3.77 (s, 3H), 3.52 (s, 4H), 2.92 (t,  $J = 6.7$  Hz, 2H), 2.68 (d,  $J = 10.8$  Hz, 2H), 1.84 (t,  $J = 6.7$  Hz, 2H), 1.69 (t,  $J = 10.6$  Hz, 2H), 1.34 (s, 6H), 1.02 (d,  $J = 6.2$  Hz, 6H).  $^{13}\text{C}$  NMR (150 MHz,  $\text{CDCl}_3$ )  $\delta$  159.83, 154.12, 148.82, 139.08, 134.07, 129.59, 126.36, 124.63, 124.49, 119.40, 115.79, 114.39, 114.28, 113.29, 112.72, 105.54, 73.85, 71.94 (2C), 69.98, 61.86, 59.52 (2C), 55.24, 32.73, 26.80 (2C), 19.59, 19.17 (2C). ESI-MS  $m/z$  calcd for  $\text{C}_{30}\text{H}_{38}\text{NO}_4$   $[\text{M} + \text{H}]^+$  476.3, found 476.4.

#### 4.1.28.3.

(2*S*,6*R*)-4-((2,2-Dimethyl-7-((4-(trifluoromethyl)benzyl)oxy)-3,4-dihydro-2*H*-benzo[*h*]chromen-5-yl)methyl)-2,6-dimethylmorpholine (**WL13**)

White solid, yield 30%, mp 150-152 °C,  $R_f = 0.66$  (petroleum ether/EtOAc = 10:1),  $[\alpha]_D^{25} = -25.00$  (C=1,  $\text{CH}_3\text{OH}$ ). HPLC purity 95.35% (A%/B% = 2:98,  $R_t = 4.355$  min).  $^1\text{H}$  NMR (400 MHz,  $\text{DMSO}-d_6$ )  $\delta$  7.79 (d,  $J = 8.1$  Hz, 2H), 7.74 (d,  $J = 8.2$  Hz, 2H), 7.63 (d,  $J = 8.7$  Hz, 2H), 7.30 (t,  $J = 8.0$  Hz, 1H), 6.99 (d,  $J = 7.7$  Hz, 1H), 5.42 (s, 2H), 3.52 (d,  $J = 12.6$  Hz, 4H), 2.94 (t,  $J = 6.7$  Hz, 2H), 2.68 (d,  $J = 10.7$  Hz, 2H), 1.85 (t,  $J = 6.7$  Hz, 2H), 1.71 (t,  $J = 10.6$  Hz, 2H), 1.35 (s, 6H), 1.02 (d,  $J = 6.2$  Hz, 6H).  $^{13}\text{C}$  NMR (150 MHz,  $\text{CDCl}_3$ )  $\delta$  153.70, 148.90, 141.50, 134.33, 128.31, 127.18 (2C), 126.39, 125.55, 125.53, 124.52, 124.38, 115.94, 114.78 (2C), 113.95, 105.52, 73.93, 71.95 (2C), 69.25, 61.84, 59.51 (2C), 32.70, 26.79 (2C), 19.60, 19.16 (2C). ESI-MS  $m/z$  calcd for  $\text{C}_{30}\text{H}_{35}\text{F}_3\text{NO}_3$   $[\text{M} + \text{H}]^+$  514.2, found 514.5.

#### 4.1.29. 7-(Benzyloxy)-2,2-dimethyl-2*H*-benzo[*h*]chromene-5-carbohydrazide (**21**)

A solution of **13** (5.00 g, 12.87 mmol) in hydrazine hydrate (30 mL) was stirred and refluxed for 8 h. The reaction solution was concentrated to produce the crude product **21** as yellow oil (4.87g, 98%), which was used directly for the next step without purification.

#### 4.1.30. 2-(7-(Benzyloxy)-2,2-dimethyl-2*H*-benzo[*h*]chromen-5-yl)-1,3,4-oxadiazole (**22**)

The above crude product **21** (4.87 g, 13.01 mmol) was dissolved in triethyl orthoformate (9.64 g, 65.05 mmol), which was refluxed for 12 h. The reaction mixture was then cooled to room temperature, the solvent was removed under reduced pressure, and the residue was purified by flash column chromatography (petroleum ether/EtOAc) to afford **22** as yellow solid (2.98, 60%). mp 198-200 °C, ESI-MS  $m/z$  calcd for  $\text{C}_{24}\text{H}_{21}\text{N}_2\text{O}_3$   $[\text{M} + \text{H}]^+$  385.1, found 385.3.

#### 4.1.31. 2,2-Bimethyl-5-(1,3,4-oxadiazol-2-yl)-3,4-dihydro-2*H*-benzo[*h*]chromen-7-ol (**23**)

The preparation method of **23** was similar to that of **16a**. Yellow solid, mp 203-205 °C, ESI-MS  $m/z$  calcd for

$C_{17}H_{17}N_2O_3$  [M + H]<sup>+</sup> 297.1, found 297.4.

#### 4.1.32. General procedure for the preparation of the 2H-benzo[h]chromene derivatives **WK1-WK9**

The preparation method of **WK1-WK9** was similar to that of **WL1-WL10**.

##### 4.1.32.1. 2-(7-(Benzyloxy)-2,2-dimethyl-3,4-dihydro-2H-benzo[h]chromen-5-yl)-1,3,4-oxadiazole (**WK1**)

White solid, yield 66%, mp 150-152 °C,  $R_f$  = 0.57 (petroleum ether/EtOAc = 10:1). HPLC purity 97.55% (A%/B% = 2:98,  $R_t$  = 2.819 min). <sup>1</sup>H NMR (400 MHz, DMSO-*d*<sub>6</sub>) δ 9.35 (s, 1H), 8.34 (s, 1H), 7.72 (d, *J* = 8.5 Hz, 1H), 7.59–7.48 (m, 3H), 7.47–7.40 (m, 2H), 7.40–7.33 (m, 1H), 7.15 (d, *J* = 7.7 Hz, 1H), 5.34 (s, 2H), 3.19 (t, *J* = 6.7 Hz, 2H), 1.92 (t, *J* = 6.7 Hz, 2H), 1.41 (s, 6H). <sup>13</sup>C NMR (100 MHz, CDCl<sub>3</sub>) δ 165.20, 154.80, 152.22, 149.70, 136.88, 128.67 (2C), 128.23, 128.02, 127.46, 127.40 (2C), 124.38, 120.18, 115.90, 114.43, 114.00, 106.17, 74.56, 70.27, 32.58, 26.73 (2C), 22.43. ESI-HRMS *m/z* calcd for C<sub>24</sub>H<sub>23</sub>N<sub>2</sub>O<sub>3</sub> [M + H]<sup>+</sup> 387.1708, found 387.1780.

##### 4.1.32.2. 2-(2,2-Dimethyl-7-((4-methylbenzyl)oxy)-3,4-dihydro-2H-benzo[h]chromen-5-yl)-1,3,4-oxadiazole (**WK2**)

White solid, yield 80%, mp 120-122 °C,  $R_f$  = 0.60 (petroleum ether/EtOAc = 10:1). HPLC purity 96.73% (A%/B% = 4:96,  $R_t$  = 3.519 min). <sup>1</sup>H NMR (400 MHz, DMSO-*d*<sub>6</sub>) δ 9.34 (s, 1H), 8.32 (s, 1H), 7.71 (d, *J* = 8.5 Hz, 1H), 7.50 (t, *J* = 8.1 Hz, 1H), 7.43 (d, *J* = 7.7 Hz, 2H), 7.24 (d, *J* = 7.7 Hz, 2H), 7.14 (d, *J* = 7.7 Hz, 1H), 5.28 (s, 2H), 3.19 (t, *J* = 6.7 Hz, 2H), 2.33 (s, 3H), 1.92 (t, *J* = 6.7 Hz, 2H), 1.41 (s, 6H). <sup>13</sup>C NMR (100 MHz, CDCl<sub>3</sub>) δ 165.20, 154.88, 152.20, 149.68, 137.79, 133.83, 129.33 (2C), 128.22, 127.53 (2C), 127.47, 124.40, 120.12, 115.96, 114.31, 113.96, 106.15, 74.54, 70.22, 32.58, 26.72 (2C), 22.43, 21.26. ESI-HRMS *m/z* calcd for C<sub>25</sub>H<sub>25</sub>N<sub>2</sub>O<sub>3</sub> [M + H]<sup>+</sup> 401.1865, found 401.1862.

##### 4.1.32.3. 2-(2,2-Dimethyl-7-((2-methylbenzyl)oxy)-3,4-dihydro-2H-benzo[h]chromen-5-yl)-1,3,4-oxadiazole (**WK3**)

White solid, yield 77%, mp 176-178 °C,  $R_f$  = 0.58 (petroleum ether/EtOAc = 10:1). HPLC purity 97.67% (A%/B% = 4:96,  $R_t$  = 3.519 min). <sup>1</sup>H NMR (400 MHz, DMSO-*d*<sub>6</sub>) δ 9.33 (s, 1H), 8.30 (s, 1H), 7.73 (d, *J* = 8.5 Hz, 1H), 7.58–7.47 (m, 2H), 7.32–7.18 (m, 4H), 5.32 (s, 2H), 3.19 (t, *J* = 6.7 Hz, 2H), 2.39 (s, 3H), 1.92 (t, *J* = 6.7 Hz, 2H), 1.41 (s, 6H). <sup>13</sup>C NMR (100 MHz, CDCl<sub>3</sub>) δ 165.16, 154.92, 152.21, 149.72, 136.87, 134.65, 130.49, 128.64, 128.34, 128.23, 127.47, 126.07, 124.37, 120.19, 115.83, 114.41, 114.02, 106.00, 74.56, 68.99, 32.58, 26.73 (2C), 22.43, 19.03. ESI-HRMS *m/z* calcd for C<sub>25</sub>H<sub>25</sub>N<sub>2</sub>O<sub>3</sub> [M + H]<sup>+</sup> 401.1865, found 401.1866.

##### 4.1.32.4. 2-(7-((3-Methoxybenzyl)oxy)-2,2-dimethyl-3,4-dihydro-2H-benzo[h]chromen-5-yl)-1,3,4-oxadiazole (**WK4**)

White solid, yield 81%, mp 158-160 °C,  $R_f$  = 0.63 (petroleum ether/EtOAc = 10:1). HPLC purity 96.60% (A%/B% = 4:96,  $R_t$  = 3.221 min). <sup>1</sup>H NMR (400 MHz, DMSO-*d*<sub>6</sub>) δ 9.36 (s, 1H), 8.36 (s, 1H), 7.72 (d, *J* = 8.5 Hz, 1H), 7.51 (t, *J* = 8.1 Hz, 1H), 7.35 (t, *J* = 7.9 Hz, 1H), 7.16–7.07 (m, 3H), 6.93 (dd, *J* = 8.3, 2.5 Hz, 1H), 5.32 (s, 2H), 3.78 (s, 3H), 3.19 (t, *J* = 6.7 Hz, 2H), 1.93 (t, *J* = 6.7 Hz, 2H), 1.41 (s, 6H). <sup>13</sup>C NMR (100 MHz, CDCl<sub>3</sub>) δ 165.20, 159.87, 154.76, 152.20, 149.71, 138.50, 129.72, 128.22, 127.46, 124.38, 120.17, 119.54, 115.89, 114.45, 114.00, 113.46, 112.84, 106.22, 74.56, 70.16, 55.26, 32.58, 26.73 (2C), 22.43. ESI-HRMS *m/z* calcd for C<sub>25</sub>H<sub>25</sub>N<sub>2</sub>O<sub>4</sub> [M + H]<sup>+</sup> 417.1814, found 417.1824.

##### 4.1.32.5. 4-(((2,2-Dimethyl-5-(1,3,4-oxadiazol-2-yl)-3,4-dihydro-2H-benzo[h]chromen-7-yl)oxy)methyl)Benzonitrile (**WK5**)

White solid, yield 53%, mp 195-197 °C,  $R_f$  = 0.53 (petroleum ether/EtOAc = 10:1). HPLC purity 99.49% (A%/B% = 4:96,  $R_t$  = 2.381 min).  $^1\text{H}$  NMR (400 MHz,  $\text{DMSO}-d_6$ )  $\delta$  9.37 (s, 1H), 8.36 (s, 1H), 7.95–7.87 (m, 2H), 7.78–7.70 (m, 3H), 7.50 (t,  $J$  = 8.1 Hz, 1H), 7.11 (d,  $J$  = 7.7 Hz, 1H), 5.48 (s, 2H), 3.19 (t,  $J$  = 6.7 Hz, 2H), 1.93 (t,  $J$  = 6.7 Hz, 2H), 1.41 (s, 6H).  $^{13}\text{C}$  NMR (100 MHz,  $\text{CDCl}_3$ )  $\delta$  165.14, 154.11, 152.28, 149.83, 142.27, 132.55 (2C), 128.27, 127.55 (2C), 127.25, 124.21, 120.51, 118.66, 115.48, 115.08, 114.23, 111.88, 106.15, 74.69, 69.19, 32.52, 26.72 (2C), 22.40. ESI-HRMS  $m/z$  calcd for  $\text{C}_{25}\text{H}_{22}\text{N}_3\text{O}_3$   $[\text{M} + \text{H}]^+$  412.1661, found 412.1661.

4.1.32.6. 2-(2,2-Dimethyl-7-((4-nitrobenzyl)oxy)-3,4-dihydro-2H-benzo[h]chromen-5-yl)-1,3,4-oxadiazole (**WK6**)

Yellow solid, yield 58%, mp 197-199 °C,  $R_f$  = 0.50 (petroleum ether/EtOAc = 10:1). HPLC purity 97.28% (A%/B% = 10:90,  $R_t$  = 2.817 min).  $^1\text{H}$  NMR (600 MHz,  $\text{CDCl}_3$ )  $\delta$  8.55 (s, 1H), 8.52 (s, 1H), 8.33–8.27 (m, 2H), 7.91 (d,  $J$  = 8.5 Hz, 1H), 7.70 (d,  $J$  = 8.7 Hz, 2H), 7.44 (t,  $J$  = 8.1 Hz, 1H), 6.87 (d,  $J$  = 7.7 Hz, 1H), 5.40 (s, 2H), 3.35 (t,  $J$  = 6.8 Hz, 2H), 1.98 (t,  $J$  = 6.7 Hz, 2H), 1.48 (s, 6H).  $^{13}\text{C}$  NMR (150 MHz,  $\text{CDCl}_3$ )  $\delta$  165.11, 154.06, 152.30, 149.85, 147.67, 144.25, 128.28, 127.62 (2C), 127.24, 124.20, 123.96 (2C), 120.54, 115.44, 115.16, 115.08, 114.27, 106.17, 74.70, 68.96, 32.52, 26.72 (2C), 22.40. ESI-HRMS  $m/z$  calcd for  $\text{C}_{24}\text{H}_{22}\text{N}_3\text{O}_5$   $[\text{M} + \text{H}]^+$  431.1559, found 432.1585.

4.1.32.7. 2-(7-((4-Fluorobenzyl)oxy)-2,2-dimethyl-3,4-dihydro-2H-benzo[h]chromen-5-yl)-1,3,4-oxadiazole (**WK7**)

White solid, yield 64%, mp 166-168 °C,  $R_f$  = 0.61 (petroleum ether/EtOAc = 10:1). HPLC purity 98.77% (A%/B% = 10:90,  $R_t$  = 4.564 min).  $^1\text{H}$  NMR (600 MHz,  $\text{CDCl}_3$ )  $\delta$  8.53 (s, 1H), 8.50 (s, 1H), 7.89 (d,  $J$  = 8.5 Hz, 1H), 7.51 (dd,  $J$  = 8.4, 5.5 Hz, 2H), 7.46 (t,  $J$  = 8.1 Hz, 1H), 7.13 (t,  $J$  = 8.7 Hz, 2H), 6.92 (d,  $J$  = 7.6 Hz, 1H), 5.26 (s, 2H), 3.34 (t,  $J$  = 6.8 Hz, 2H), 1.98 (t,  $J$  = 6.8 Hz, 2H), 1.48 (s, 6H).  $^{13}\text{C}$  NMR (150 MHz,  $\text{CDCl}_3$ )  $\delta$  165.18, 163.36, 161.73, 154.63, 152.23, 149.73, 132.60, 132.58, 129.25, 128.23, 127.39, 124.35, 120.26, 115.67, 115.53, 114.60, 114.06, 106.15, 74.59, 69.64, 32.56, 26.72 (2C), 22.41. ESI-HRMS  $m/z$  calcd for  $\text{C}_{24}\text{H}_{22}\text{FN}_2\text{O}_3$   $[\text{M} + \text{H}]^+$  405.1614, found 405.1650.

4.1.32.8. 2-(7-((2,4-Dichlorobenzyl)oxy)-2,2-dimethyl-3,4-dihydro-2H-benzo[h]chromen-5-yl)-1,3,4-oxadiazole (**WK8**)

White solid, yield 67%, mp 142-144 °C,  $R_f$  = 0.59 (petroleum ether/EtOAc = 10:1). HPLC purity 99.83% (A%/B% = 2:98,  $R_t$  = 10.541 min).  $^1\text{H}$  NMR (600 MHz,  $\text{CDCl}_3$ )  $\delta$  8.55 (s, 1H), 8.53 (s, 1H), 7.91 (d,  $J$  = 8.5 Hz, 1H), 7.58 (d,  $J$  = 8.3 Hz, 1H), 7.48 (d,  $J$  = 2.1 Hz, 1H), 7.45 (t,  $J$  = 8.1 Hz, 1H), 7.31 (dd,  $J$  = 8.3, 2.1 Hz, 1H), 6.89 (d,  $J$  = 7.7 Hz, 1H), 5.35 (s, 2H), 3.35 (t,  $J$  = 6.8 Hz, 2H), 1.98 (t,  $J$  = 6.8 Hz, 2H), 1.49 (s, 6H).  $^{13}\text{C}$  NMR (150 MHz,  $\text{CDCl}_3$ )  $\delta$  165.17, 154.17, 152.27, 149.80, 134.27, 133.33, 133.16, 129.58, 129.36, 128.27, 127.43, 127.36, 124.26, 120.40, 115.62, 114.95, 114.14, 106.28, 74.63, 66.92, 32.55, 26.73(2C), 22.41. ESI-HRMS  $m/z$  calcd for  $\text{C}_{24}\text{H}_{21}\text{Cl}_2\text{N}_2\text{O}_3$   $[\text{M} + \text{H}]^+$  455.0929, found 455.0944.

4.1.32.9. 2-(7-((4-Bromobenzyl)oxy)-2,2-dimethyl-3,4-dihydro-2H-benzo[h]chromen-5-yl)-1,3,4-oxadiazole (**WK9**)

White solid, yield 58%, mp 162-164 °C,  $R_f$  = 0.66 (petroleum ether/EtOAc = 10:1). HPLC purity 100.00% (A%/B% = 10:90,  $R_t$  = 6.337 min).  $^1\text{H}$  NMR (600 MHz,  $\text{CDCl}_3$ )  $\delta$  8.53 (s, 1H), 8.50 (d,  $J$  = 0.8 Hz, 1H), 7.91–7.87 (m, 1H), 7.59–7.55 (m, 2H), 7.45 (dd,  $J$  = 8.5, 7.7 Hz, 1H), 7.41 (d,  $J$  = 8.4 Hz, 2H), 6.91–6.88 (m, 1H), 5.24 (s, 2H), 3.35 (t,  $J$  = 6.8 Hz, 2H), 1.98 (t,  $J$  = 6.8 Hz, 2H), 1.48 (s, 6H).  $^{13}\text{C}$  NMR (150 MHz,  $\text{CDCl}_3$ )  $\delta$  165.15, 154.50, 152.24, 149.75, 135.87, 131.82 (2C), 129.07 (2C), 128.23, 127.36, 124.30, 121.96, 120.30, 115.70, 114.69, 114.10, 106.16, 74.60, 69.55, 32.56, 26.72 (2C), 22.42. ESI-HRMS  $m/z$  calcd for  $\text{C}_{24}\text{H}_{22}\text{BrN}_2\text{O}_3$   $[\text{M} + \text{H}]^+$  465.0814, found 465.0829.

## 4.2. Antibacterial evaluation

### 4.2.1. Antimicrobial assays

Antimicrobial assays were performed applying the two-fold broth dilution method as previously described by our group [33, 34].

### 4.2.2 Checkerboard titration assay

Possible synergism of the tested compounds with antimicrobials were evaluated by checkerboard titration assay as previously described by our group [33-35].

### 4.2.3. Nile red efflux assay

Nile red efflux assay was carried out to assess the ability of the tested compounds to inhibit efflux as previously described by our group [33-35].

### 4.2.4. Nitrocefin uptake assay

The influence of the tested compounds on outer membrane permeability of *E. coli* BW25513 was investigated by nitrocefin uptake assay as previously described by our group [33, 34].

### 4.2.5. Measurement of the electrochemical gradient over the inner membrane

The effect of the tested compounds on pmf across the inner-membrane was evaluated by applying the DiOC<sub>2</sub>(3) fluorescent method as previously described by our group [33, 34].

## Declaration of competing interest

The authors declare that this study was carried out only with public funding. There is no funding or no agreement with commercial for profit firms.

## Acknowledgments

This research was supported financially by the National Natural Science Foundation of China (81973179, 81673284 and 81903449), the National Health and Medical Research Council of Australia (GN1147538), Key research and development project of Shandong Province (2017CXGC1401), Major Project of Research and development of Shandong Province (2019GSF108051), and the China-Australia Centre for Health Sciences Research (CACHSR no. 2019GJ05). RA is the recipient of a PhD scholarship from the Government of Saudi Arabia.

## References

- [1] M. Zwama, S. Yamasaki, R. Nakashima, K. Sakurai, K. Nishino, A. Yamaguchi, Multiple entry pathways within the efflux transporter AcrB contribute to multidrug recognition, *Nat. Commun.* 9 (2018) 124.
- [2] X.Z. Li, P. Plesiat, H. Nikaido, The challenge of efflux-mediated antibiotic resistance in Gram-negative bacteria, *Clin. Microbiol. Rev.* 28 (2015) 337-418.
- [3] O. Lomovskaya, H.I. Zgurskaya, M. Totrov, W.J. Watkins, Waltzing transporters and 'the dance macabre' between humans and bacteria, *Nat. Rev. Drug Discov.* 6 (2007) 56-65.
- [4] C.F. Higgins, Multiple molecular mechanisms for multidrug resistance transporters, *Nature* 446 (2007) 749-757.
- [5] S. Gibbons, J. Leimkugel, M. Oluwatuyi, M. Heinrich, Activity of *Zanthoxylum clava-herculis* extracts against multi-drug resistant methicillin-resistant *Staphylococcus aureus* (mdr-MRSA), *Phytother. Res.* 17 (2003) 274-275.
- [6] C.I. Kang, S.H. Kim, W.B. Park, K.D. Lee, H.B. Kim, E.C. Kim, M.D. Oh, K.W. Choe, Bloodstream infections caused by antibiotic-resistant gram-negative bacilli: risk factors for mortality and impact of inappropriate initial antimicrobial therapy on outcome, *Antimicrob. Agents Chemother.* 49 (2005) 760-766.
- [7] Y. Wang, R. Mowla, S. Ji, L. Guo, M.A. De Barros Lopes, C. Jin, D. Song, S. Ma, H. Venter, Design, synthesis and biological activity evaluation of novel 4-substituted 2-naphthamide derivatives as AcrB inhibitors, *Eur. J. Med. Chem.* 143 (2018) 699-709.
- [8] H. Venter, Reversing resistance to counter antimicrobial resistance in the World Health Organisation's critical priority of most dangerous pathogens, *Biosci. Rep.* 39 (2019) BSR20180474.
- [9] A.H. Delcour, Outer membrane permeability and antibiotic resistance, *Biochim. Biophys. Acta* 1794 (2009) 808-816.
- [10] G. Krishnamoorthy, J.W. Weeks, Z. Zhang, C.E. Chandler, H. Xue, H.P. Schweizer, R.K. Ernst, H.I. Zgurskaya, Efflux pumps of *Burkholderia thailandensis* control the permeability barrier of the outer membrane, *Antimicrob. Agents Chemother.* 63 (2019) e00956-19.
- [11] A.V. Vargiu, H. Nikaido, Multidrug binding properties of the AcrB efflux pump characterized by molecular dynamics simulations, *Proc. Natl. Acad. Sci. U. S. A.* 109 (2012) 20637-20642.
- [12] H. Nikaido, J.M. Pages, Broad-specificity efflux pumps and their role in multidrug resistance of Gram-negative bacteria, *FEMS Microbiol. Rev.* 36 (2012) 340-363.
- [13] K. Poole, R. Srikumar, Multidrug efflux in *Pseudomonas aeruginosa*: components, mechanisms and clinical significance, *Curr. Top. Med. Chem.* 1 (2001) 59-71.
- [14] M. Arzanlou, W.C. Chai, H. Venter, Intrinsic, adaptive and acquired antimicrobial resistance in Gram-negative

bacteria, *Essays Biochem.* 61 (2017) 49-59.

[15] R. Nakashima, K. Sakurai, S. Yamasaki, K. Hayashi, C. Nagata, K. Hoshino, Y. Onodera, K. Nishino, A. Yamaguchi, Structural basis for the inhibition of bacterial multidrug exporters, *Nature* 500 (2013) 102-106.

[16] S. Jamshidi, J.M. Sutton, K.M. Rahman, An overview of bacterial efflux pumps and computational approaches to study efflux pump inhibitors, *Future Med. Chem.* 8 (2016) 195-210.

[17] X. Wen, A.M. Langevin, M.J. Dunlop, Antibiotic export by efflux pumps affects growth of neighboring bacteria, *Sci. Rep.* 8 (2018) 15120.

[18] T.J. Opperman, S.T. Nguyen, Recent advances toward a molecular mechanism of efflux pump inhibition, *Front. Microbiol.* 6 (2015) 421.

[19] T.J. Opperman, S.M. Kwasny, H.S. Kim, S.T. Nguyen, C. Houseweart, S. D'Souza, G.C. Walker, N.P. Peet, H. Nikaido, T.L. Bowlin, Characterization of a novel pyranopyridine inhibitor of the AcrAB efflux pump of *Escherichia coli*, *Antimicrob. Agents Chemother.* 58 (2014) 722-733.

[20] V.K. Ramaswamy, P. Cacciotto, G. Mallocci, A.V. Vargiu, P. Ruggerone, Computational modelling of efflux pumps and their inhibitors, *Essays Biochem.* 61 (2017) 141-156.

[21] J.M. Blair, G.E. Richmond, L.J. Piddock, Multidrug efflux pumps in Gram-negative bacteria and their role in antibiotic resistance, *Future Microbiol.* 9 (2014) 1165-1177.

[22] N. Abdali, J.M. Parks, K.M. Haynes, J.L. Chaney, A.T. Green, D. Wolloscheck, J.K. Walker, V.V. Rybenkov, J. Baudry, J.C. Smith, H.I. Zgurskaya, Reviving antibiotics: efflux pump inhibitors that interact with AcrA, a membrane fusion protein of the AcrAB-TolC multidrug efflux pump, *ACS infect. dis.* 3 (2017) 89-98.

[23] K. Poole, Efflux-mediated multiresistance in Gram-negative bacteria, *Clin. Microbiol. Infect.* 10 (2004) 12-26.

[24] P. Hinchliffe, M.F. Symmons, C. Hughes, V. Koronakis, Structure and operation of bacterial tripartite pumps, *Annu. Rev. Microbiol.* 67 (2013) 221-242.

[25] D. Du, Z. Wang, N.R. James, J.E. Voss, E. Klimont, T. Ohene-Agyei, H. Venter, W. Chiu, B.F. Luisi, Structure of the AcrAB-TolC multidrug efflux pump, *Nature* 509 (2014) 512-515.

[26] T. Eicher, M.A. Seeger, C. Anselmi, W. Zhou, L. Brandstatter, F. Verrey, K. Diederichs, J.D. Faraldo-Gomez, K.M. Pos, Coupling of remote alternating-access transport mechanisms for protons and substrates in the multidrug efflux pump AcrB, *Elife* 3 (2014) e03145.

[27] A. Yamaguchi, R. Nakashima, K. Sakurai, Structural basis of RND-type multidrug exporters, *Front. Microbiol.* 6 (2015) 327.

[28] H. Venter, R. Mowla, T. Ohene-Agyei, S. Ma, RND-type drug efflux pumps from Gram-negative bacteria: molecular

mechanism and inhibition, *Front. Microbiol.* 6 (2015) 377.

[29] S. Murakami, R. Nakashima, E. Yamashita, T. Matsumoto, A. Yamaguchi, Crystal structures of a multidrug transporter reveal a functionally rotating mechanism, *Nature* 443 (2006) 173-179.

[30] R. Nakashima, K. Sakurai, S. Yamasaki, K. Nishino, A. Yamaguchi, Structures of the multidrug exporter AcrB reveal a proximal multisite drug-binding pocket, *Nature* 480 (2011) 565-569.

[31] H. Sjuts, A.V. Vargiu, S.M. Kwasny, S.T. Nguyen, H.S. Kim, X. Ding, A.R. Ornik, P. Ruggerone, T.L. Bowlin, H. Nikaido, K.M. Pos, T.J. Opperman, Molecular basis for inhibition of AcrB multidrug efflux pump by novel and powerful pyranopyridine derivatives, *Proc. Natl. Acad. Sci. U. S. A.* 113 (2016) 3509-3514.

[32] T. Eicher, H.J. Cha, M.A. Seeger, L. Brandstatter, J. El-Delik, J.A. Bohnert, W.V. Kern, F. Verrey, M.G. Grutter, K. Diederichs, K.M. Pos, Transport of drugs by the multidrug transporter AcrB involves an access and a deep binding pocket that are separated by a switch-loop, *Proc. Natl. Acad. Sci. U. S. A.* 109 (2012) 5687-5692.

[33] Y. Wang, R. Mowla, L. Guo, A.D. Ogunniyi, T. Rahman, M.A. De Barros Lopes, S. Ma, H. Venter, Evaluation of a series of 2-naphthamide derivatives as inhibitors of the drug efflux pump AcrB for the reversal of antimicrobial resistance, *Bioorg. Med. Chem. Lett.* 27 (2017) 733-739.

[34] T. Ohene-Agyei, R. Mowla, T. Rahman, H. Venter, Phytochemicals increase the antibacterial activity of antibiotics by acting on a drug efflux pump, *Microbiologyopen* 3 (2014) 885-896.

[35] Y. Wang, R. Alenzy, D. Song, X. Liu, Y. Teng, R. Mowla, Y. Ma, S.W. Polyak, H. Venter, S. Ma, Structural optimization of natural product nordihydroguaretic acid to discover novel analogues as AcrB inhibitors, *Eur. J. Med. Chem.* (2019) 111910.

[36] O. Lomovskaya, M.S. Warren, A. Lee, J. Galazzo, R. Fronko, M. Lee, J. Blais, D. Cho, S. Chamberland, T. Renau, R. Leger, S. Hecker, W. Watkins, K. Hoshino, H. Ishida, V.J. Lee, Identification and characterization of inhibitors of multidrug resistance efflux pumps in *Pseudomonas aeruginosa*: novel agents for combination therapy, *Antimicrobial agents and chemotherapy* 45 (2001) 105-116.

[37] J.A. Bohnert, B. Karamian, H. Nikaido, Optimized Nile Red efflux assay of AcrAB-TolC multidrug efflux system shows competition between substrates, *Antimicrob. Agents Chemother.* 54 (2010) 3770-3775.

[38] H.I. Zgurskaya, H. Nikaido, Bypassing the periplasm: reconstitution of the AcrAB multidrug efflux pump of *Escherichia coli*, *Proc. Natl. Acad. Sci. U. S. A.* 96 (1999) 7190-7195.

[39] J.A. Bohnert, S. Schuster, W.V. Kern, T. Karcz, A. Olejarz, A. Kaczor, J. Handzlik, K. Kiec-Kononowicz, Novel piperazine arylideneimidazolones inhibit the AcrAB-TolC pump in *Escherichia coli* and simultaneously act as fluorescent membrane probes in a combined real-time influx and efflux assay, *Antimicrob. Agents Chemother.* 60 (2016) 1974-1983.

Journal Pre-proof

**Fig. 1.** Structures of some representative AcrB inhibitors.

**Fig. 2.** Structure-based design of novel AcrB inhibitors.

**Fig. 3.** Inhibition of Nile Red efflux. Wild-type resistant cells with active pump (solid black line), (-)AcrB drug-sensitive cells (grey line) or wild-type cells in the presence of the tested compounds (dotted lines) were preloaded with Nile Red before the start of fluorescence measurements. Efflux was triggered at 100 sec by the addition of 0.2% glucose (indicated by arrow). Representative fluorescent traces are shown for triplicate experiments with different batches of cells.

**Fig. 4.** The effect of the tested compounds on outer membrane permeability. *E. coli* were treated with 10  $\mu$ M CCCP to inhibit the efflux of nitrocefin. Nitrocefin was added to the cells that received no compound (blue circles), cells treated with the outer membrane permeabilizer polymyxin B (red squares) or the test compounds (red triangles). Nitrocefin hydrolysis by the periplasmic  $\beta$ -lactamase was observed as an increase in absorbance at 490 nm. Representative traces are shown from duplicate experiments performed on different days.

**Fig. 5.** The effect of the tested compounds on membrane potential ( $\Delta\psi$ ) across the inner-membrane. Bacterial suspensions were either left untreated (solid blue line) or exposed to 8-128  $\mu$ g/mL test compounds (broken red line) for 10 min after which the potentiometric probe, DiOC<sub>2</sub>(3) was added and the fluorescence monitored until it plateaued. Cells were then re-energized with 0.5% glucose and the establishment of a membrane potential (inside negative) was measured as an increase in fluorescence until it plateaued. The membrane potential was then disrupted by the addition of the proton ionophore CCCP (observed as a sharp drop in fluorescence intensity).

**Fig. 6.** *In silico* docking studies. The molecular interactions of AcrB with (a) **WK2** and (b) **WL10**.

**Scheme 1.** Reagents and conditions: (a) ZnCl<sub>2</sub>, POCl<sub>3</sub>, 50 °C, 3 h; (b) dibromoethane, K<sub>2</sub>CO<sub>3</sub>, CH<sub>3</sub>CN, 75 °C, 8 h; (c) corresponding alkylamine, K<sub>2</sub>CO<sub>3</sub>, DMF, 78 °C, 6 h; (d) chloroacetic chloride, Et<sub>3</sub>N, 0 °C to r.t., 2 h; (e) K<sub>2</sub>CO<sub>3</sub>, DMF, 75 °C, 5 h.

**Scheme 2.** Reagents and conditions: (a) BnCl, K<sub>2</sub>CO<sub>3</sub>, DMF, reflux, 4 h; (b) diethyl succinate, EtONa, EtOH, reflux, 6 h; (c) (CH<sub>3</sub>CO)<sub>2</sub>O, NaOAc, r.t.; (d) K<sub>2</sub>CO<sub>3</sub>, MeOH; (e) PhB(OH)<sub>2</sub>, AcOH, toluene, reflux, 34 h.

**Scheme 3.** Reagents and conditions: (a) NaOH, 70 °C, 6 h; (b) corresponding alkylamine, TBTU, DIEA, CH<sub>3</sub>CN, r.t.; (c) Pd/C, H<sub>2</sub>, MeOH/EtOAc, r.t.; (d) substituted benzyl chloride or bromide, K<sub>2</sub>CO<sub>3</sub>, CH<sub>3</sub>CN, 55 °C, 4-8 h; (e) LiAlH<sub>4</sub>, THF, 0 °C to r.t., 2 h; (f) PPh<sub>3</sub>, CBr<sub>4</sub>, DCM, 0 °C to r.t., 3 h; (g) corresponding alkylamine, K<sub>2</sub>CO<sub>3</sub>, DMF, 70 °C, 6 h; (h) hydrazine hydrate, reflux, 3 h; (i) triethyl orthoformate, reflux, 12 h.

**Table 1.** The synergistic effect of the active compounds in WH-WJ series with different antibacterials against wild-type drug-resistant strain *E. coli* BW25113 expressing AcrB (indicated as (+)AcrB).

Compound	Concentration ( $\mu\text{g}/\text{mL}$ )	MIC ( $\mu\text{g}/\text{mL}$ )					Compound	Concentration ( $\mu\text{g}/\text{mL}$ )	MIC ( $\mu\text{g}/\text{mL}$ )				
		CAM	ERY	TPP	LEV	RIF			CAM	ERY	TPP	LEV	RIF
WH3	8	8	64	1024	0.03	16	WJ5	8	8	64	1024	0.06	16
	16	8	64	1024	0.03	16		16	8	64	1024	0.06	16
	32	8	64	1024	0.03	16		32	8	64	1024	0.06	16
	64	8	64	1024	0.03	16		64	8	64	1024	0.06	16
	128	8	64	1024	0.03	16		128	4	32	1024	0.06	16
WH4	8	8	64	512	0.06	16	WJ6	8	8	64	1024	0.06	16
	16	8	64	512	0.06	16		16	8	64	1024	0.06	16
	32	8	64	512	0.03	16		32	8	64	1024	0.06	16
	64	8	64	512	0.03	16		64	8	64	1024	0.06	16
	128	8	64	512	0.03	16		128	8	64	512	0.06	16
WH8	8	8	64	1024	0.06	16	WJ7	8	8	64	1024	0.06	16
	16	8	64	1024	0.06	16		16	8	64	1024	0.06	16
	32	8	64	512	0.06	16		32	8	64	1024	0.06	16
	64	4	64	256	0.06	16		64	4	64	1024	0.06	16
	128	N/D	N/D	N/D	N/D	16		128	4	32	1024	0.06	16
W17	8	8	64	1024	0.03	16	WJ10	8	8	64	1024	0.06	16
	16	8	64	1024	0.03	16		16	8	64	1024	0.06	16
	32	8	64	1024	0.03	16		32	4	32	1024	0.06	16
	64	8	64	1024	0.03	16		64	4	32	1024	0.06	16
	128	8	64	1024	0.03	16		128	4	32	1024	0.06	16
W18	8	8	64	1024	0.06	16	NDGA	16	8	64	1024	0.06	16
	16	8	64	1024	0.06	16		32	8	64	1024	0.06	16
	32	8	64	1024	0.06	16		64	8	64	1024	0.03	16
	64	8	64	1024	0.06	16		128	4	64	128	0.03	16
	128	8	32	512	0.06	16		256	2	32	64	0.03	16
WJ1	8	8	64	1024	0.06	16	A3	256	8	64	512	0.06	16
	16	8	64	1024	0.06	16		512	4	32	256	0.06	16
	32	8	64	1024	0.06	16	NONE (+)AcrB	0	8	64	1024	0.06	16
	64	4	64	1024	0.06	16	NONE (-) AcrB	0	2	4	32	0.04	16
	128	4	64	1024	0.03	16							

CAM = Chloramphenicol; ERY = Erythromycin; TPP = Tetraphenylphosphonium; LEV = levofloxacin; RIF = Rifampicin

**Table 2.** The synergistic effect of the active compounds in WK and WL series) with different antibacterials against wild-type drug-resistant strain *E. coli* BW25113 expressing AcrB (indicated as (+)AcrB).

Compound	Concentration ( $\mu\text{g/mL}$ )	MIC ( $\mu\text{g/mL}$ )					Compound	Concentration ( $\mu\text{g/mL}$ )	MIC ( $\mu\text{g/mL}$ )				
		CAM	ERY	TPP	LEV	RIF			CAM	ERY	TPP	LEV	RIF
WK1	8	8	64	512	0.06	16	WL1	8	8	64	1024	0.06	16
	16	8	64	512	0.06	16		16	8	64	1024	0.06	16
	32	4	32	512	0.06	16		32	8	64	512	0.06	16
	64	4	32	512	0.06	16		64	4	64	256	0.01	16
	128	2	16	128	0.06	16		128	1	32	64	0.01	16
WK2	8	8	32	512	0.03	16	WL2	8	8	64	1024	0.06	16
	16	8	32	512	0.03	16		16	8	64	1024	0.06	16
	32	8	32	512	0.03	16		32	8	32	1024	0.06	16
	64	8	16	512	0.03	16		64	4	32	512	0.06	16
	128	2	8	64	0.01	16		128	4	16	256	0.06	16
WK3	8	8	64	512	0.06	16	WL7	8	8	64	512	0.03	16
	16	8	64	512	0.06	16		16	4	64	512	0.03	16
	32	8	32	512	0.06	16		32	4	64	512	0.03	16
	64	8	32	512	0.06	16		64	4	16	512	0.03	16
	128	8	16	256	0.06	16		128	4	8	64	0.03	16
WK4	8	8	64	1024	0.06	16	WL8	8	4	64	512	0.06	16
	16	8	64	1024	0.06	16		16	4	64	512	0.06	16
	32	8	64	1024	0.06	16		32	4	32	512	0.06	16
	64	8	64	512	0.06	16		64	4	32	256	0.06	16
	128	8	32	512	0.06	16		128	2	16	128	0.06	16
WK5	8	8	64	1024	0.06	16	WL9	8	8	64	512	0.06	16
	16	4	64	1024	0.06	16		16	8	64	512	0.06	16
	32	4	64	1024	0.06	16		32	8	64	512	0.06	16
	64	4	64	512	0.06	16		64	8	16	512	0.06	16
	128	2	32	512	0.06	16		128	4	16	256	0.06	16
WK6	8	8	64	1024	0.06	16	WL10	8	4	16	512	0.06	16
	16	8	64	1024	0.06	16		16	4	16	512	0.06	16
	32	8	64	1024	0.06	16		32	4	16	256	0.06	16
	64	8	32	1024	0.06	16		64	4	16	128	0.06	16
	128	4	32	1024	0.06	16		128	2	8	64	0.01	16
WK7	8	8	64	1024	0.06	16	NDGA	16	8	64	1024	0.06	16
	16	8	64	512	0.06	16		32	8	64	1024	0.06	16
	32	8	32	512	0.06	16		64	8	64	1024	0.03	16
	N/D	N/D	N/D	N/D	N/D	16		128	4	64	128	0.03	16
	128	N/D	N/D	N/D	N/D	16		256	2	32	64	0.03	16
NONE (+)AcrB	0	8	64	1024	0.06	16	A3	256	4	32	512	0.06	16
NONE (-) AcrB	0	2	4	32	0.04	16		512	4	16	256	0.06	16

CAM = Chloramphenicol; ERY = Erythromycin; TPP = Tetraphenylphosphonium; LEV = levofloxacin; RIF = Rifampicin

**Table 3.** In vitro cytotoxicity profiles of **WK2** and **WL7** against HepG2 cells.

Compounds	% Inhibition	% Inhibition
	(10 uM)	(100 uM)
<b>WK2</b>	6	87
<b>WL7</b>	2	66
Paclitaxel	IC <sub>50</sub> =12.6 nM	

**Table 4.** Summary of biological activities of the active chromanone and 2*H*-benzo[h]chromene derivatives.

Compd	MIC (μg/mL)		Antimicrobial sensitizing activity (vs antibacterials)	Does not increase antimicrobial activity of RIF	Inhibition of AcrB efflux (μM)	No outer membrane damage	No inner membrane damage
	WT	(-)AcB					
WH3	>512	>128	L	✓	100	✓	✓
WH4	>512	>128	T, L	✓	200	✓	✓
WH8	>512	>128	C, T	✓	200	✓	✓
WI8	>512	>128	L	✓	100	✓	✓
WI9	>512	>128	E, T	✓	100	✓	✓
WJ1	>512	>128	C, L	✓	100	✓	✓
WJ5	>512	>128	C, E	✓	100	✓	✓
WJ6	>512	>128	T	✓	100	✓	✓
WJ7	>512	>128	C, E	✓	200	✓	✓
WJ10	>512	>128	C, E	✓	50	✓	✓
WK1	>512	>128	C, E, T	✓	100	✓	✓
WK2	>512	>128	C, E, T, L	✓	100	✓	✓
WK3	>512	>128	E, T	✓	100	✓	✓
WK4	>512	>128	E, T	✓	>100	✓	✓
WK5	>512	>128	C, E, T	✓	50	✓	✓
WK6	>512	>128	C, E	✓	100	✓	✓
WK7	64	64	C, E, T	✓	50	✓	✓
WL1	>512	>128	C, E, T, L	✓	100	✓	✗
WL2	>512	>128	C, E, T	✓	100	✓	✓
WL7	>512	>128	C, E, T, L	✓	100	✓	✓
WL8	>512	>128	C, E, T	✓	50	✓	✓
WL9	>512	>128	C, E, T	✓	50	✓	✓
WL10	>512	>128	C, E, T, L	✓	100	✓	✓

C = chloramphenicol, E = erythromycin, L = Levofloxacin, T = tetraphenylphosphonium

Fig. 1

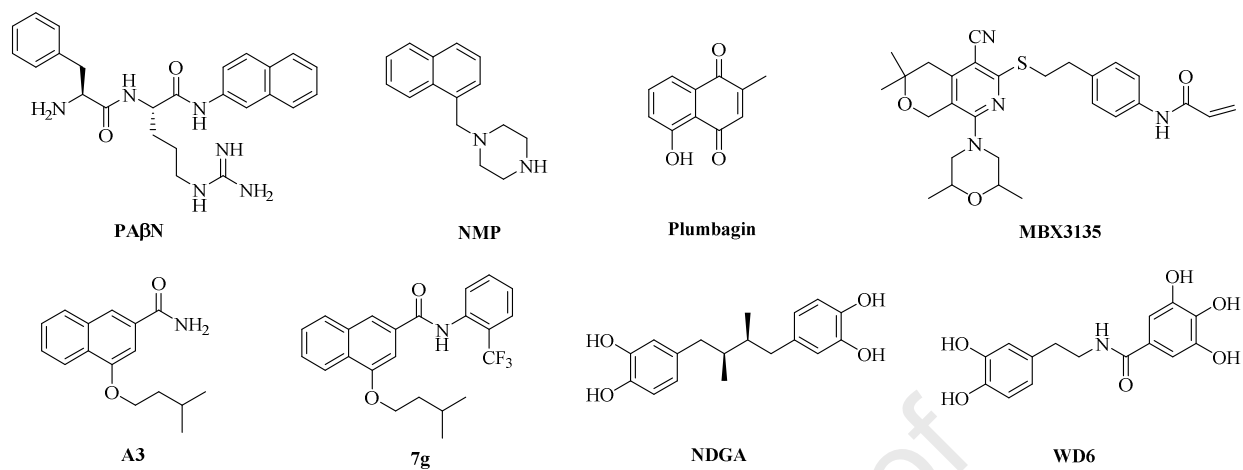
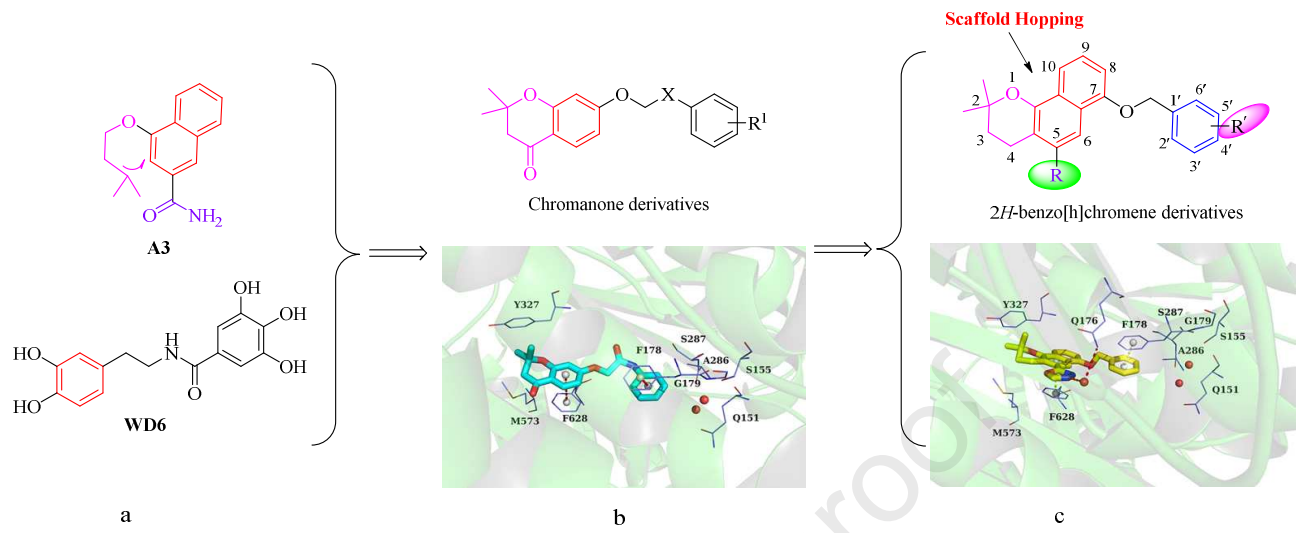
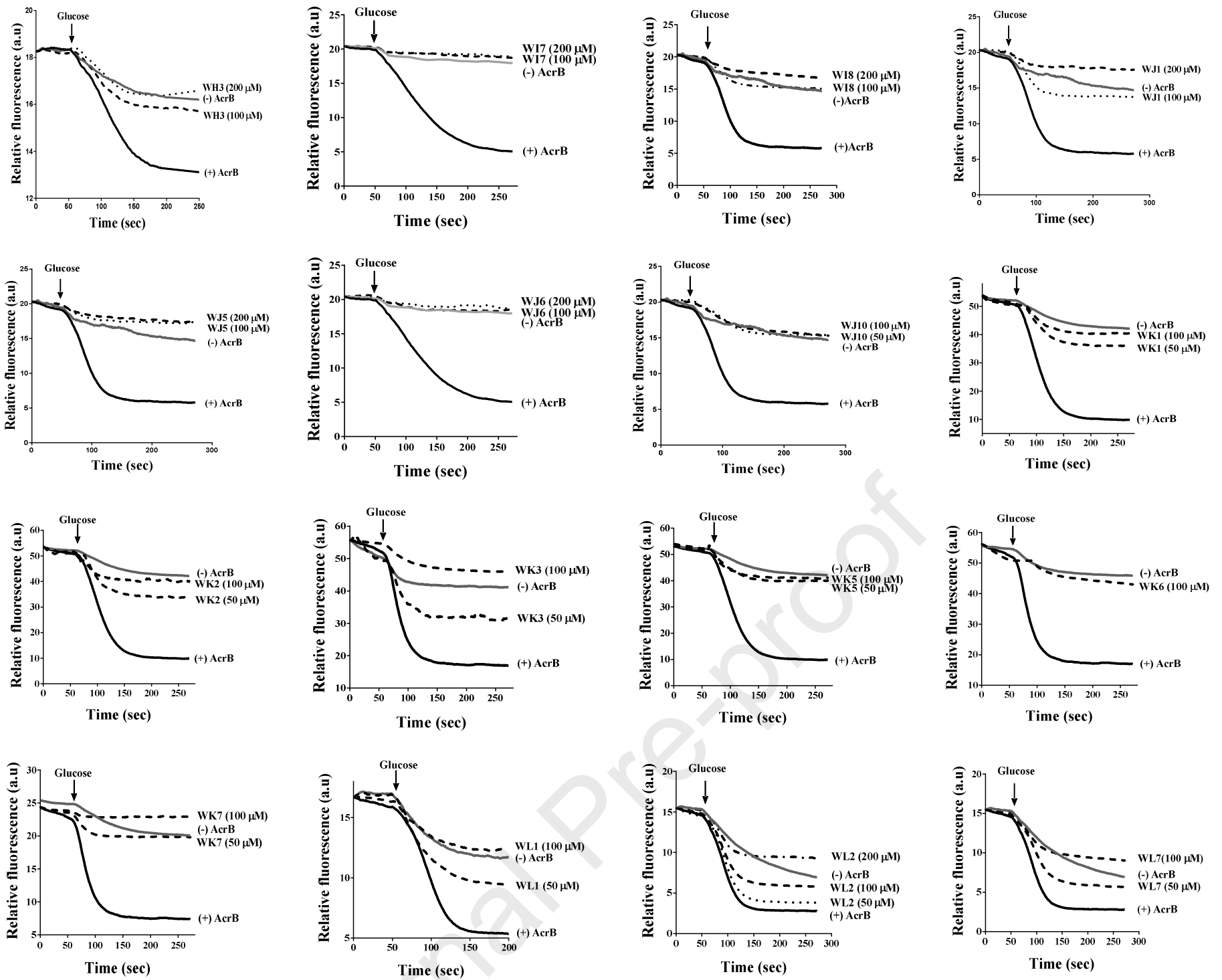
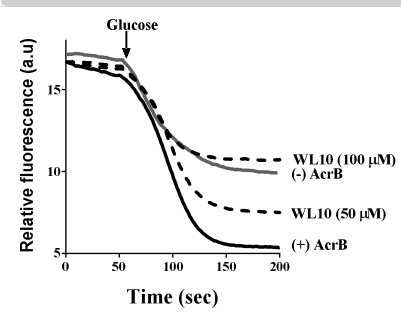
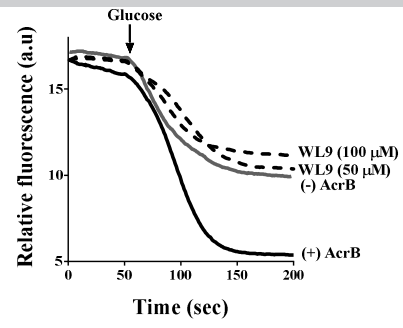
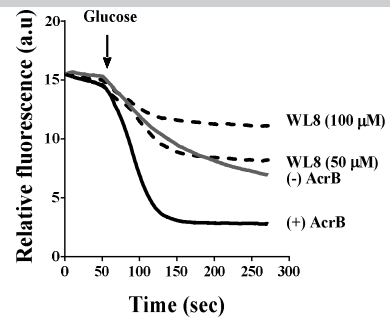


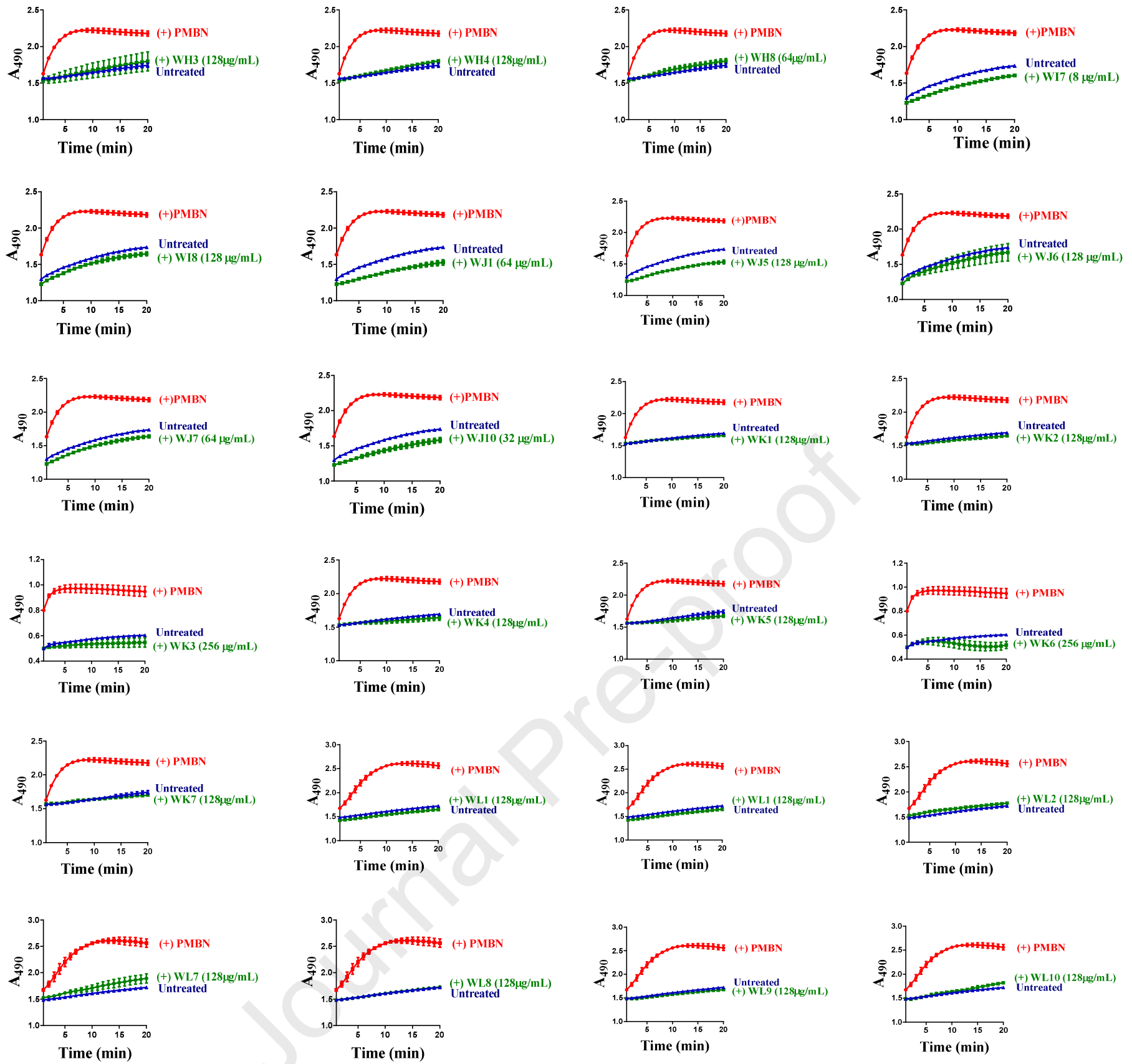
Fig. 2







Journal Pre-proof



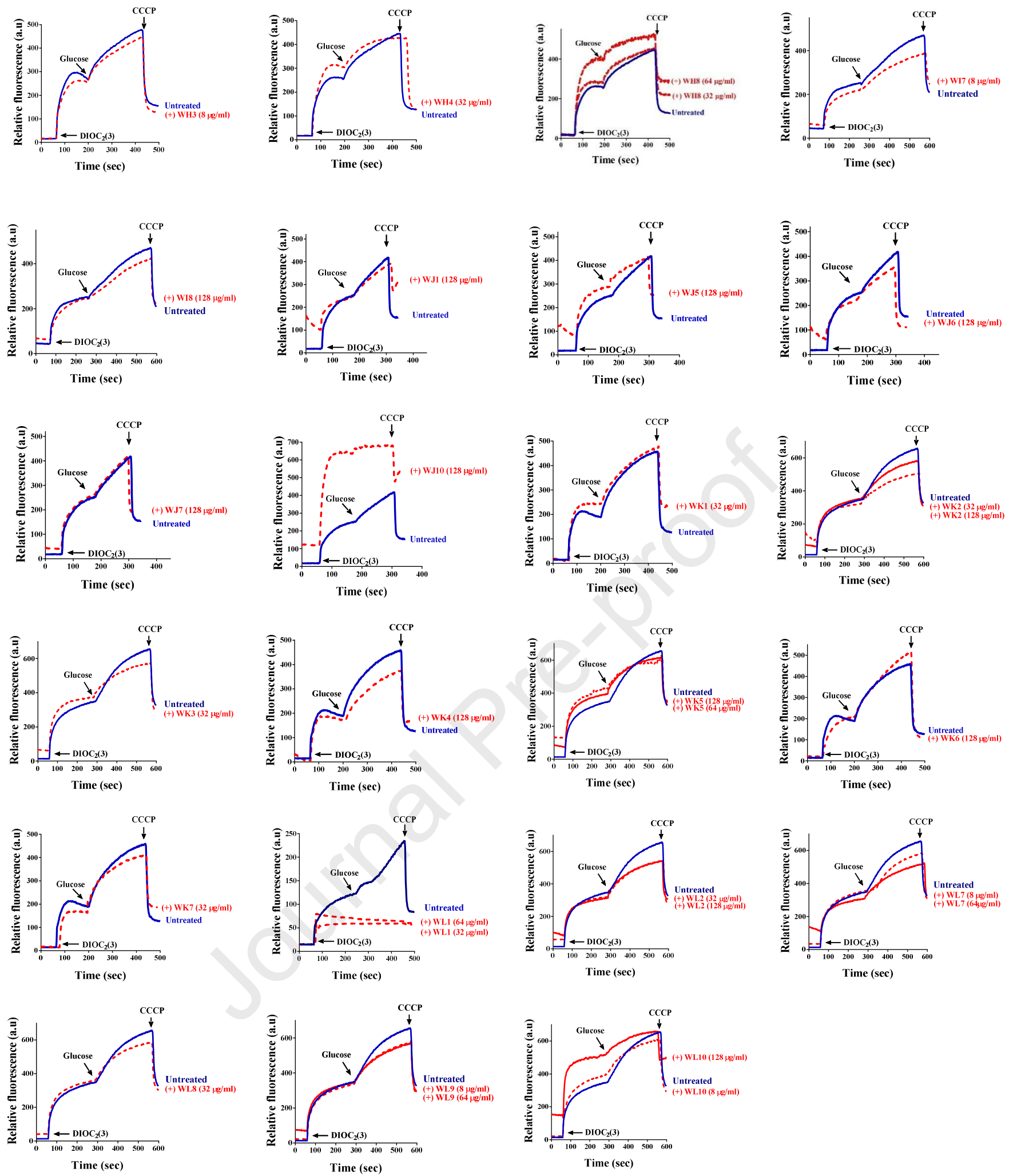
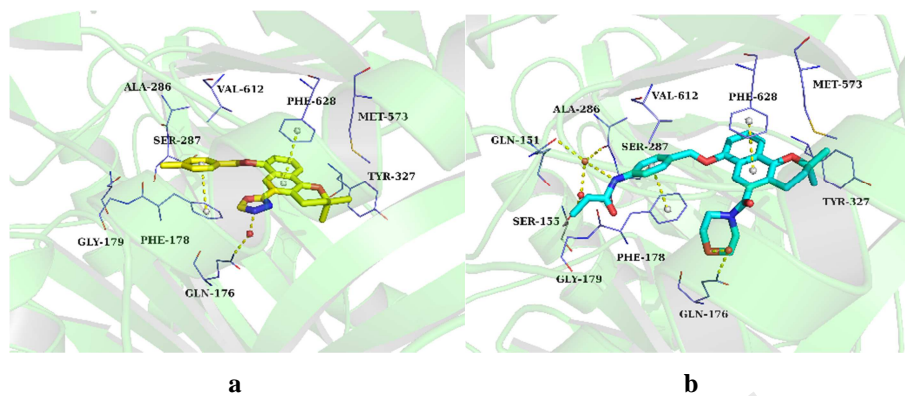
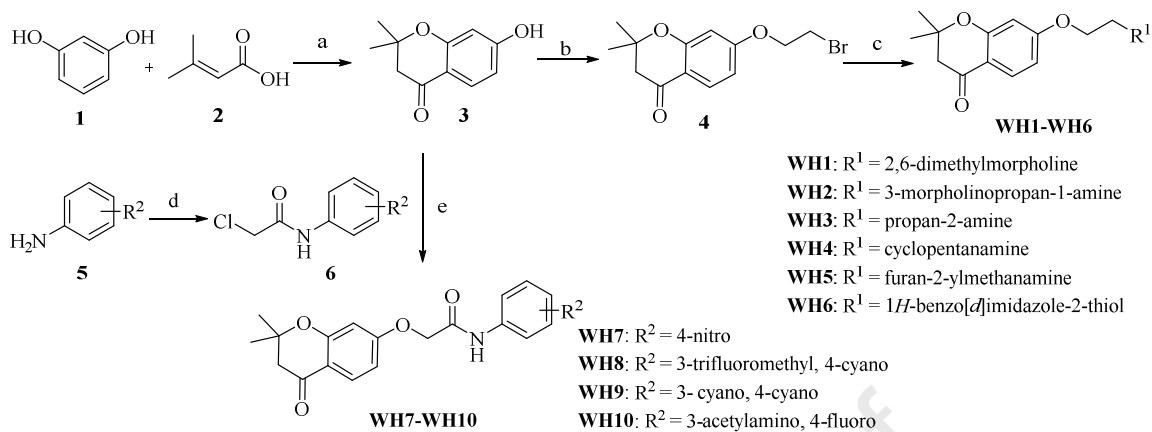


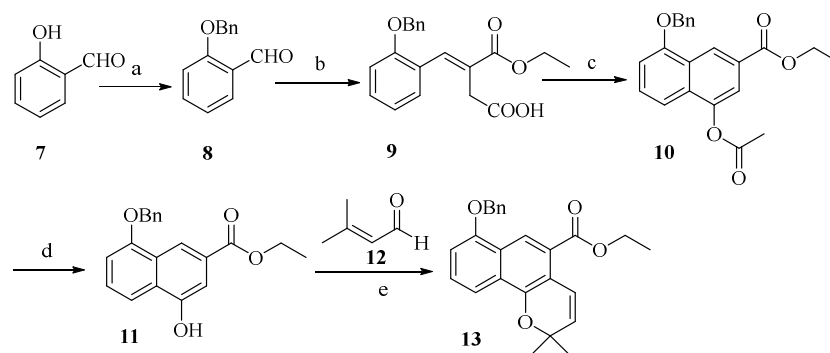
Fig. 6



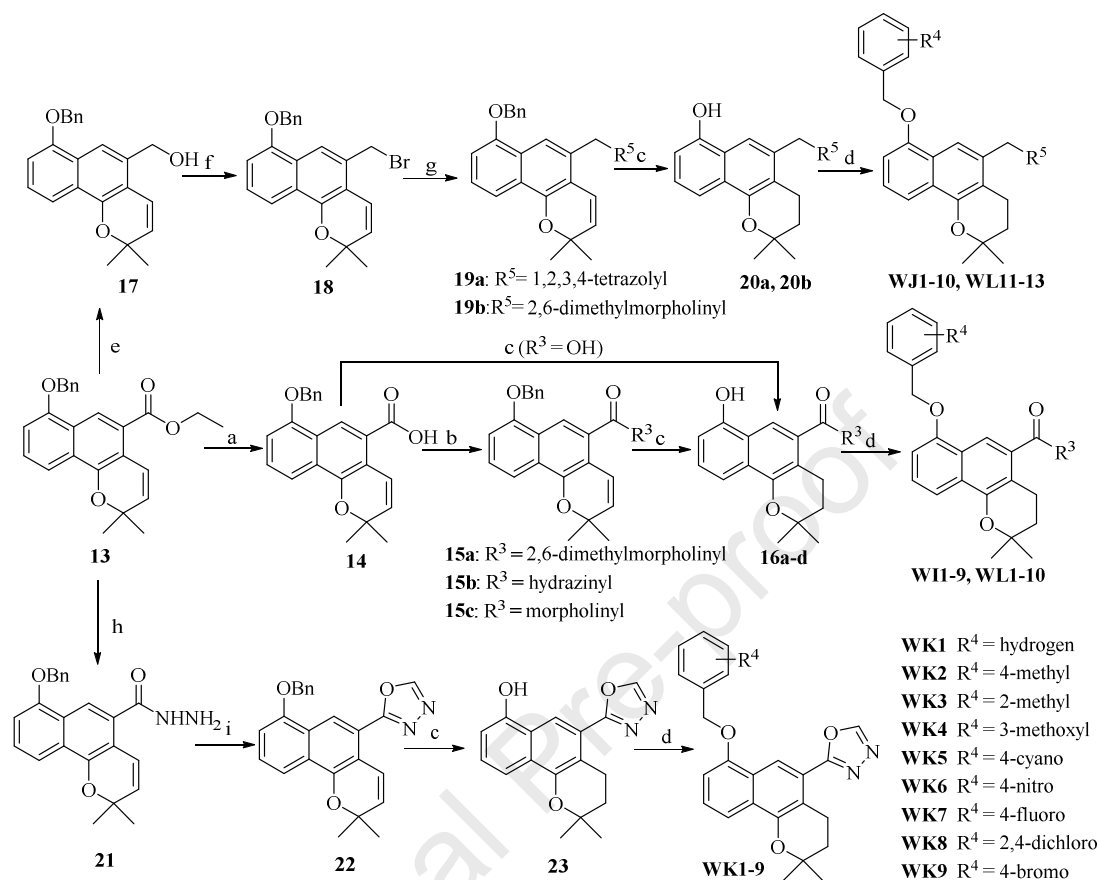
Scheme 1



Scheme 2



Scheme 3



**WJ1** R<sup>3</sup> = 2,6-dimethylmorpholinyl, R<sup>4</sup> = 4-methyl  
**WJ2** R<sup>3</sup> = 2,6-dimethylmorpholinyl, R<sup>4</sup> = 4-tert-butyl  
**WJ3** R<sup>3</sup> = 2,6-dimethylmorpholinyl, R<sup>4</sup> = 3-methoxy  
**WJ4** R<sup>3</sup> = 2,6-dimethylmorpholinyl, R<sup>4</sup> = 4-cyano  
**WJ5** R<sup>3</sup> = 2,6-dimethylmorpholinyl, R<sup>4</sup> = 4-fluoro  
**WJ6** R<sup>3</sup> = 2,6-dimethylmorpholinyl, R<sup>4</sup> = 2,4-dichloro  
**WJ7** R<sup>3</sup> = 2,6-dimethylmorpholinyl, R<sup>4</sup> = 2,6-dichloro  
**WJ8** R<sup>3</sup> = 2,6-dimethylmorpholinyl, R<sup>4</sup> = 4-bromo  
**WJ9** R<sup>3</sup> = 2,6-dimethylmorpholinyl, R<sup>4</sup> = 4-nitro  
**WJ10** R<sup>3</sup> = 2,6-dimethylmorpholinyl, R<sup>4</sup> = 4-methyl  
**WJ11** R<sup>3</sup> = 2,6-dimethylmorpholinyl, R<sup>4</sup> = 4-tert-butyl  
**WJ12** R<sup>3</sup> = 2,6-dimethylmorpholinyl, R<sup>4</sup> = 3-methoxy  
**WJ13** R<sup>3</sup> = 2,6-dimethylmorpholinyl, R<sup>4</sup> = 4-cyano

**WJ8** R<sup>5</sup> = 1,2,3,4-tetrazolyl, R<sup>4</sup> = 4-*N*-isopropylcarbamoyl  
**WJ9** R<sup>5</sup> = 1,2,3,4-tetrazolyl, R<sup>4</sup> = 4-acetylamino  
**WJ10** R<sup>5</sup> = 1,2,3,4-tetrazolyl, R<sup>4</sup> = 4-acrylamido  
**WL1** R<sup>3</sup> = hydroxyl, R<sup>4</sup> = hydrogen  
**WL2** R<sup>3</sup> = hydroxyl, R<sup>4</sup> = 3-methoxy  
**WL3** R<sup>3</sup> = hydroxyl, R<sup>4</sup> = 4-acetylamino  
**WL4** R<sup>3</sup> = hydrazinyl, R<sup>4</sup> = hydrogen  
**WL5** R<sup>3</sup> = hydrazinyl, R<sup>4</sup> = 3-methoxy  
**WL6** R<sup>3</sup> = hydrazinyl, R<sup>4</sup> = 4-acetylamino  
**WL7** R<sup>3</sup> = morpholinyl, R<sup>4</sup> = hydrogen  
**WL8** R<sup>3</sup> = morpholinyl, R<sup>4</sup> = 3-methoxy  
**WL9** R<sup>3</sup> = morpholinyl, R<sup>4</sup> = 4-trifluoromethyl  
**WL10** R<sup>3</sup> = morpholinyl, R<sup>4</sup> = 4-acrylamido  
**WL11** R<sup>5</sup> = 2,6-dimethylmorpholinyl, R<sup>4</sup> = hydrogen  
**WL12** R<sup>5</sup> = 2,6-dimethylmorpholinyl, R<sup>4</sup> = 3-methoxy  
**WL13** R<sup>5</sup> = 2,6-dimethylmorpholinyl, R<sup>4</sup> = 4-trifluoromethyl

> Novel chromanone and 2*H*-benzo[*h*]chromene derivatives were designed and synthesized. > They were evaluated to inhibit AcrB efflux pump. > Twenty-four compounds were found to increase the efficacy of antibiotics tested. > **WK2**, **WL7** and **WL10** possessed broad-spectrum and high-efficiency EPI activity. > Those compounds had favorable properties as potential AcrB inhibitors.

Journal Pre-proof

**Declaration of Interest Statement**

The authors declare that this study was carried out only with public funding. There is no funding or no agreement with commercial for profit firms.

Journal Pre-proof